Excitation spectrum of doped two-leg ladders: A field theory analysis

D. Controzzi[1] and A. M. Tsvelik[2]
[1]*International School for Advanced Studies and INFN, via Beirut 4, 34014 Trieste, Italy*
[2]*Department of Physics, Brookhaven National Laboratory, Upton, New York 11973-5000, USA*
(Received 3 March 2005; published 8 July 2005)

We apply quantum field theory to study the excitation spectrum of doped two-leg ladders. It follows from our analysis that throughout most of the phase diagram the spectrum consists of degenerate quartets of kinks and antikinks and a multiplet of vector particles split according to the symmetry of the problem as 3+2+1. This basic picture experiences corrections when one moves through the phase diagram. In some regions the splitting may become very small and in others it is so large that some multiplets are pushed in the continuum and become unstable. At second-order transition lines masses of certain particles vanish. Very close to the first-order transition line additional generations of particles emerge. Strong interactions in some sectors may generate additional bound states (like breathers) in the asymmetric charge sector. We briefly describe the properties of various correlation functions in different phases.

DOI: 10.1103/PhysRevB.72.035110 PACS number(s): 71.10.Pm, 11.10.Kk, 72.80.Sk

I. INTRODUCTION

The problem of ladderlike materials has attracted a lot of attention since the original paper by Dagotto and Rice.[1] Important experimental realizations of two-leg ladder systems include, for example, the famous "telephone number" compound $Sr_{14-x}Ca_xCu_{24}O_{41}$ which has a spin gap and exhibits a transition from charge density wave (CDW) to superconducting (SC) state under the increase of Ca concentration.[2–9] Besides the experimental relevance the study of this problem gives rise to many questions of rather general character. Even if ladder systems represent only the first step from a purely one-dimensional world into higher dimensions, this step introduces a lot of new interesting physics. In addition, the problem of doped spin ladders is just a particular case of a more general problem of multiorbital quasi-one-dimensional models[10] and an increase in the number of orbitals dramatically increases the complexity of the lattice Hamiltonian, raising legitimate questions about universality.

In this paper we focus on the problem of doped two-leg ladders. Assuming that the spectral gaps are much smaller than the bandwidth (the applicability of these assumption to real systems is discussed at the end of the paper), we study the low-energy physics using the field theory approach. The intensive theoretical research conducted on this subject at the last eight years has established the following facts.

(A) *Strong-weak tunneling duality*. The form of the effective action describing the low-energy behavior of the system is independent (up to a simple operator transformation) on whether one takes into account the interchain tunneling or considers just the interchain interactions. One arrives at this conclusion comparing effective actions derived in the limit of strong tunneling (see, for example, Refs. 11–14) with the theories derived in the limit of weak tunneling.[15,16] The strong-weak tunneling duality may be a boon for numerical calculations, allowing one to extract information about the excitation spectrum in the one-parameter range by performing actual calculations in the other.

(B) *Superconductivity-CDW duality*. The phase diagram includes the Tomonaga-Luttinger- (TL-) type phase as well as phases with spectral gaps. The only stable TL phase is the one where all modes are gapless. As soon as an attractive interaction appears in one channel it induces an attraction in all other ones, generating spectral gaps for all modes except the symmetric charge mode. The strong-coupling phases are characterized by power-law correlations for particular operators (order parameters). These phases are classified either as SC or CDW. For the two-chain model there are two SC phases (s and d) and two CDW phases (also s and d, the latter phase also being known as Orbital Antiferromagnet (OAF)[17] or staggered flux[18] phase). Such classification is valid only for a weak repulsion when the Luttinger parameter K_c, characterizing the gapless charge mode, is close to 1. At $K_c < 1/2$ the Wigner crystal phase with $4k_F$ density correlations competes with the SC phases.[19,20] The low-energy Hamiltonians in different sectors differ by the sign of certain coupling constants and transform into each other by canonical transformations of the fields. These transformations realize the authomorphisms of the O(6) group.[16]

(C) *Emergent attractive interactions*. As follows both from the numerical[22,23] and analytic calculations based on a renormalization group (RG) analysis,[12,13,16,21,24,25] the system at low energies may enter into a strong-coupling regime even if all bare couplings are repulsive. In that case the system passes through an intermediate weak-coupling regime. If E^* is the energy at which the weak coupling is reached, then it can be shown that the strong-coupling regime is achieved at energies of the order of E^{*2}/Λ, where Λ is the bare ultraviolet cutoff. It is probably safe to say that the emergent attraction leads to small gaps.

It was first suggested in Ref. 12 that if the bare couplings are not very large, the low-energy sector of a two-leg ladder is described by a universal Hamiltonian with a symmetry larger than the symmetry of the lattice model. This corresponds to the $O(6)\times U(1)$ symmetry in the doped case and the O(8) symmetry at half filling. The original suggestion was based on the observation that the RG flows of different coupling constants converge in the strong-coupling limit to the same asymptotics corresponding to a higher symmetry.

Convergence of RG flows has also been found to occur in other systems[25] and is frequently associated with dynamical symmetry enlargement (DSE). A careful discussion of DSE for some specific models can be found in Ref. 26. This problem is addressed also here matching the RG analysis, valid at weak coupling, with methods valid at strong coupling. The conclusion is that in models where the number of particle flavors is not large, there are conditions when one may indeed expect a small splitting of particle multiplets. Such conditions exist in systems with weak backscattering, like carbon nanotubes.

The goal of this paper is to use a quantum field theory approach to describe the phase diagram and excitation spectrum of a doped two-leg Hubbard-type model. We combine the RG methods with methods suitable to study the strong-coupling limit, like the $1/N$ expansion,[27] exact solutions, and perturbation theory around specific integrable points in the parameter space of the effective field theory.[28] We also discuss the conditions of validity of the field theory description. As said above, this description is valid when the correlation length is much larger than the ultraviolet (UV) cutoff. This regime is known as the *scaling limit*.

The paper is organized as follows. In the next section we introduce the effective low-energy description of doped two-leg ladders, the so-called generalized O(6) Gross-Neveu (GN) model, and briefly analyze the RG equations. In Sec. III we discuss the possible strong-coupling phases of the model, and in Sec. IV we describe its symmetries and identify the phase boundaries. The spectrum of generalized Gross-Neveu models is discussed in Sec. V using the large-N approximation. Some specific points of the phase diagram are described by integrable models with the O(6) GN model being the most prominent. These integrable points are identified in Sec. VI. In the vicinity of these points we study the spectrum using a specific strong-coupling perturbation theory described in Sec. VII. The spectrum close to the phase boundaries is summarized in Sec. VIII. Section IX is devoted to the study of a simplified $[\mathrm{O}(3)\times\mathrm{O}(3)]$-symmetric model where the RG equations can be integrated explicitly. In Sec. X we briefly consider the structure of some correlation functions. We summarize the main results and discuss the experimental relevance in the last section. The paper has several appendixes.

II. MODEL

The model in its original formulation includes electron creation and annihilation operators $c^{\dagger}_{i,l,\sigma}$, $c_{i,l,\sigma}$ labeled by chain indices, $l=1,2$, and spin indices, $\sigma=+1$, for spin up ($\uparrow$) and $\sigma=-1$ for spin down ($\downarrow$). For instance, the extended Hubbard model has the standard form

$$H=-t_{\parallel}\sum_{i,l,\sigma}(c^{\dagger}_{i,l,\sigma}c_{i+1,l,\sigma}+\mathrm{H.c.})+U\sum_{i,l}n_{i,l,\uparrow}n_{i,l,\downarrow}-t_{\perp}\sum_{i,l,\sigma}(c^{\dagger}_{i,1,\sigma}c_{i,2,\sigma}+\mathrm{H.c.})+V_{\parallel}\sum_{i,l}n_{i,l}n_{i+i,l}+V_{\perp}\sum_{i,l}n_{i,1}n_{i,2}, \tag{1}$$

where, as usual, the parameters $t_{\parallel}$ and $t_{\perp}$ are the hopping matrix elements along and between the chains, U is the on-site repulsion, and $V_{\parallel}$ and $V_{\perp}$ are the next-nearest-neighbor interactions, with $n_{i,l,\sigma}=c^{\dagger}_{i,l,\sigma}c_{i,l,\sigma}$ and $n_{i,l}=n_{i,l,\uparrow}+n_{i,l,\downarrow}$. The lattice Hamiltonian (1) has a $\mathrm{U}(1)\times\mathrm{SU}(2)\times\mathbb{Z}_2$ symmetry. If necessary, one can include also exchange interactions.

A. Low-energy field theory

As we have mentioned in the Introduction, the effective field theory, describing the low-energy behavior of the Hamiltonian (1), is largely independent of whether one considers strong interactions and weak interchain tunneling, as was done, for example, in Refs. 15 and 16, or diagonalizes the interchain hopping first and treats the bare interactions as weak, as has been done in the majority of other papers. To be precise, there are two differences: (i) in one case the fields are labeled by chain indices and in the other by transverse wave vectors $q=0,\pi$, and (ii) the Hamiltonians of both sectors are related to each other by the particle-hole transformation.

As far as the analysis of the phase diagram and the spectrum are concerned, it is more advantageous to have a low-energy description in the Majorana fermion representation. The Majorana formulation is derived by bosonization and subsequent refermionization of the original Hamiltonian (the procedure was introduced in Ref. 29; see also Ref. 30) and, for the specific model (1), can be found, for instance, in Refs. 14 and 19. Away from half-filling, the resulting low-energy field theory consists of two parts: one contains a decoupled symmetric charge mode $\Phi^{(+)}_c$ and the other contains all other fields. The latter can be written in terms of six Majorana fermions as

$$H=H_0+V, \tag{2a}$$

where H_0 is the free part,

$$H_0=-\frac{\mathrm{i}}{2}\sum_{a=1}^{3}v_s(\chi^a_R\partial_x\chi^a_R-\chi^a_L\partial_x\chi^a_L)-\frac{\mathrm{i}}{2}\sum_{a=1}^{3}v_a(\xi^a_R\partial_x\xi^a_R-\xi^a_L\partial_x\xi^a_L), \tag{2b}$$

and V describes the interaction between the right- and left-moving Majorana fermions $\chi^a_{R,L}$ and $\xi^a_{R,L}$:

$$\begin{aligned}V=&-g_{\sigma+}(\chi^a_R\chi^a_L)^2-g_{\rho-}[(\xi^1_R\xi^1_L)+(\xi^2_R\xi^2_L)]^2\\&-2(\chi^a_R\chi^a_L)\{g_{\sigma-}(\xi^3_R\xi^3_L)+g_{c,st}[(\xi^1_R\xi^1_L)+(\xi^2_R\xi^2_L)]\}\\&-2g_{c,ss}(\xi^3_R\xi^3_L)[(\xi^1_R\xi^1_L)+(\xi^2_R\xi^2_L)]\end{aligned} \tag{2c}$$

(summation over repeated indices is assumed). The symmetry of the continuum Hamiltonian is $\mathrm{U}(1)\times\mathrm{U}(1)\times\mathrm{SU}(2)\times\mathbb{Z}_2$, being somewhat higher than the symmetry of the lattice model. As we have already mentioned, one U(1) field (the total charge mode $\Phi^{(+)}_c$) is decoupled and is not shown in the above Hamiltonian, while the second U(1) symmetry emerges only asymptotically at lower energies. The mode $\Phi^{(+)}_c$ is responsible for high conductivity along the ladders observed in $Sr_{14-x}Ca_xCu_{24}O_{41}$.[8] The SU(2) triplet χ^a and the fermion ξ^3 are made of bosonic fields of the spin sector. They reflect the $\mathrm{SU}(2)\times\mathbb{Z}_2$ symmetry of the spin sector and also

appear in the low-energy description of the two-leg Heisenberg ladder.[29] The situation here differs from the Heisenberg ladder since no explicit mass term is present in the Hamiltonian and the masses are generated dynamically. The fermionic doublet $\xi_{1,2}$ describes the asymmetric charge mode, which we will denote $\Theta_c^{(-)}$.

The original observables are nonlocal in terms of the Majorana fermions (vector particles). The latter particles, if they remain stable, represent collective excitations of the system. We emphasize that the vector multiplet in Eqs. (2) is naturally split into submultiplets as $3+1+2$. The model (2) can also be represented as six critical Ising models coupled together by products of the energy density operators. This representation is convenient because the original fermionic bilinears are local in terms of the Ising model order and disorder parameter fields. To clarify the symmetries and the structure of the model, we can rewrite it as

$$\begin{aligned} H = {} & H_{O(3)}[\chi; g_{\sigma,+}] + H_{O(2)}[\Theta_c^{(-)}; g_{\rho,-}] + H_{Ising}[\xi^3] \\ & + 2\mathrm{i}(\chi_R^a \chi_L^a)\{\mathrm{i} g_{\sigma-}(\xi_R^3 \xi_L^3) + \bar{g}_{c,st} \cos[\beta \Theta_c^{(-)}]\} \\ & + \mathrm{i} 2 g_{c,ss}(\xi_R^3 \xi_L^3) \cos[\beta \Theta_c^{(-)}]. \end{aligned} \tag{3}$$

Here H_{Ising} is the Hamiltonian of the critical Ising (CI) model and $H_{O(N)}$ represents the $O(N)$ GN model,[31] which can be described in terms of N Majorana fermions $\psi_{R,L}^a$ ($a=1,\ldots,N$) as

$$H_{O(N)}[\psi; g_N] = -\frac{\mathrm{i}}{2} v_N (\psi_R^a \partial_x \psi_R^a - \psi_L^a \partial_x \psi_L^a) - g_N (\psi_R^a \psi_L^a)^2. \tag{4}$$

The spectrum of $H_{O(N)}$ is massive for $g_N < 0$, provided $N > 2$, while $H_{O(2)}$ is always massless and is equivalent to the Gaussian model.

Though the form of the Hamiltonians (2) and (3) is fixed by the symmetry, estimates of the coupling constants are available only for weak interactions. The backscattering interactions are weak in such systems as carbon nanotubes which have the same symmetry as two-leg ladders, but not in two-leg ladders themselves. Therefore our philosophy will be the same as in the particle physics: we will express everything in terms of low-energy parameters (mass gaps) and assume these gaps to be much smaller than the ultraviolet cutoff (whatever this cutoff is). As an additional simplification we will ignore the difference between the velocities, setting $v_s = v_a = 1$.

B. Preliminary RG analysis

The first step in our analysis is to establish the conditions under which the system scales to strong coupling. To do it we use the single loop RG equations as obtained in Refs. 11, 12, 16, and 21:

$$\dot{g}_{\rho-} = -3 g_{c,st}^2 - g_{c,ss}^2, \tag{5a}$$

$$\dot{g}_{c,ss} = -g_{\rho-} g_{c,ss} - 3 g_{\sigma-} g_{c,st}, \tag{5b}$$

$$\dot{g}_{\sigma-} = -2 g_{\sigma+} g_{\sigma-} - 2 g_{c,st} g_{c,ss}, \tag{5c}$$

$$\dot{g}_{c,st} = -(g_{\rho-} + 2 g_{\sigma+}) g_{c,st} - g_{\sigma-} g_{c,ss}, \tag{5d}$$

$$\dot{g}_{\sigma+} = -g_{\sigma+}^2 - g_{\sigma-}^2 - 2 g_{c,st}^2. \tag{5e}$$

Here the overdot corresponds to a derivative in RG time $t = (4\pi v)^{-1} \ln(\Lambda/\epsilon)$. Thus small energies in our notations correspond to large t.

Further in the text we will study the RG equations close to the O(6)-symmetric point and, in more detail, for a simplified $[\mathrm{O}(3) \times \mathrm{O}(3)]$-symmetric model (cf. Sec. IX). In the latter case Eqs. (5) can be solved analytically.

It is possible to show that there are two areas of stability.

(i) The weak-coupling area, where the repulsion dominates. All couplings scale to zero. The resulting phase is the $\mathrm{O}(6) \times \mathrm{U}(1)$ TL liquid perturbed by marginally irrelevant perturbations. We found the exact boundaries of this area for the $\mathrm{O}(3) \times \mathrm{O}(3)$ model, but qualitatively one can say that the TL liquid appears as a fixed point when the diagonal interactions are repulsive and exceed the off-diagonal terms: $g_{\sigma+} \sim g_{\rho,-} > |g_{\sigma-}|, |g_{c,ss}|, |g_{c,st}|$.

(ii) The strong-coupling area. In the RG sense this area is the basin of attraction of the O(6)-symmetric point $-g_{\sigma+} = -g_{\rho,-} = |g_{\sigma-}| = |g_{c,ss}| = |g_{c,st}| > 0$. In order to get to strong coupling it is enough to have just one attractive diagonal interaction. Moreover and very intriguingly, one may even start from all interactions being repulsive. The system will scale to strong coupling anyway provided the off-diagonal interactions are sufficiently strong (this would correspond to the emergent attraction described in Introduction). This follows from the stability analysis of the unstable symmetric line $g_{\sigma+} = g_{\rho,-} = |g_{\sigma-}| = |g_{c,ss}| = |g_{c,st}| > 0$.

The RG equations determine an overall scale at which the strong coupling is achieved:

$$M = \Lambda f[g_a(0)] = \Lambda \tilde{f}(g_1(0), C_1, \ldots, C_{Q-1}). \tag{6}$$

Each set of initial conditions sets the system on a particular RG trajectory defined by its invariants C_i ($i=1,\ldots,Q-1$), where Q is the number of coupling constants. For a given set of C_i's the scaling limit exists if for an arbitrary large Λ one can choose a starting point on the trajectory such that M remains constant. It turns out that for trajectories with an emergent attraction this is not possible. Therefore the space of C_i's where the scaling limit is defined is a subspace of $(Q-1)$-dimensional space (scaling subspace). Inside of this space the masses may depend on C_i's and this dependence is not determined perturbatively. In view of this it is clear that the existence of a "strong-coupling point" or DSE requires independence (or at least weak dependence) of the mass spectrum on RG invariants. Otherwise, strongly correlated phases are not points, but have their own geography with the excitation spectrum changing throughout the phase. We will continue this discussion in Secs. VII C and IX where we consider mass variations related to small deviations from the O(6) and $\mathrm{O}(3) \times \mathrm{O}(3)$ symmetries, respectively.

III. STRONG-COUPLING PHASES AND ORDER PARAMETERS

To explore the possible phases of the model it is more convenient to use the mixed representation (2). Here the Hamiltonian is expressed in terms of bosonic fields $\Theta_c^{(\pm)}$ associated with the charge modes and Ising fields σ_a (μ_a) with $a=0,\ldots,3$ associated with the spin modes ξ^3 and χ^a, respectively. The phases of the system are in one-to-one correspondence with the field vacua. These vacua are determined by the signs of the renormalized couplings $(g_{\sigma-}, g_{c,st}, g_{c,ss})$ in the strong-coupling regime (recall that these signs may have nothing to do with signs of the bare coupling constants). The analysis of the phase diagram has already been conducted, and here we repeat many results obtained in Refs. 13, 14, 16, and 20. To keep contact with these works we use a strong-tunneling approach, introducing bonding ($p=1$) and antibonding ($p=-1$) operators

$$C(n)_{p,\sigma} = \frac{c_{n,1,\sigma} + p c_{n,2,\sigma}}{\sqrt{2}} \tag{7}$$

associated with transverse wave vectors $q=0,\pi$, respectively. The bosonization notations are given in Appendix A, and the relationship with the weak-tunneling approach is discussed at the end of the section.

When the forward scattering in the symmetric charge channel is not strong, there are four possible phases: superconducting s (SCs) and d wave (SCd), CDW, and what is now frequently called d-wave CDW (CDWd). Its order parameter is of orbital antiferromagnet[17] and staggered flux[18] type. In terms of the lattice operators the order parameters of the four phases have the form

$$\Delta_{SCs}(n) = \sum_{p=\pm 1} C(n)_{p,\sigma} C(n)_{p,-\sigma} = \sum_{p=\pm} [R_{p,\uparrow} L_{p,\downarrow} + L_{p,\uparrow} R_{p,\downarrow}], \tag{8a}$$

$$\Delta_{SCd}(n) = \sum_{p=\pm 1} \sin(\pi p/2) C(n)_{p,\sigma} C(n)_{p,-\sigma} = \sum_{p=\pm} p[R_{p,\uparrow} L_{p,\downarrow} + L_{p,\uparrow} R_{p,\downarrow}], \tag{8b}$$

$$\Delta_{CDW}(n) = \sum_{p=\pm 1,\sigma} C^\dagger(n)_{p,\sigma} C(n)_{-p,\sigma} e^{2k_F i n a_0} = \sum_{p=\pm 1,\sigma} R^+_{p,\sigma} L_{-p,\sigma}, \tag{8c}$$

$$\Delta_{CDWd}(n) = \sum_{p=\pm 1,\sigma} \sin(\pi p/2) C^\dagger(n)_{p,\sigma} C(n)_{-p,\sigma} e^{2k_F i n a_0} = \sum_{p=\pm 1,\sigma} p R^+_{p,\sigma} L_{-p,\sigma}. \tag{8d}$$

Here we introduced the right- and left-moving components of the lattice fermion operators:

$$C_{p,\sigma}(n) = e^{-i k_F^{(p)} x} R_{p,\sigma}(x) + e^{i k_F^{(p)} x} L_{p,\sigma}(x) \quad (x = n a_0), \tag{9}$$

where $k_F^{(p)}$ are Fermi vectors of the different bands and $k_F = (k_F^{(+)} + k_F^{(-)})/2 = \pi(1-\delta)/2a_0$, with δ being the doping and a_0 the lattice constant.

The SCd phase is found in the region $(+,+,+)$ and is characterized by

$$\Theta_c^{(-)} = 0, \quad \langle \sigma_a \rangle \neq 0 \quad (a = 0,1,2,3) \tag{10a}$$

or

$$\Theta_c^{(-)} = \sqrt{\pi}/2, \quad \langle \mu_a \rangle \neq 0 \quad (a = 0,1,2,3), \tag{10b}$$

where $\langle \cdots \rangle = \langle 0 | \cdots | 0 \rangle$ is the vacuum expectation value (VEV). This phase has power-law correlations (quasi-long-range order) in the d-wave Cooper channel (8b). The order parameter in the continuum limit is

$$\Delta_{SCd} \sim e^{i\sqrt{\pi}\Theta_c^{(+)}} \{\cos[\sqrt{\pi}\Theta_c^{(-)}] \sigma_1 \sigma_2 \sigma_3 \sigma_0 - i \sin[\sqrt{\pi}\Theta_c^{(-)}] \mu_1 \mu_2 \mu_3 \mu_0\}. \tag{11}$$

For $(-,+,-)$ one finds the CDWd phase, characterized by

$$\Theta_c^{(-)} = 0, \quad \langle \sigma_a \rangle \neq 0 \quad (a = 1,2,3), \quad \mu_0 \neq 0 \tag{12a}$$

or

$$\Theta_c^{(-)} = \sqrt{\pi}/2, \quad \langle \mu_a \rangle \neq 0 \quad (a = 1,2,3), \quad \sigma_0 \neq 0. \tag{12b}$$

One gets to this phase from the first one through a $\mathbb{Z}_2$ QCP. In the continuum Eq. (8d) becomes

$$\Delta_{CDWd} \sim e^{-i\sqrt{\pi}\Phi_c^{(+)}} \{i \sin[\sqrt{\pi}\Theta_c^{(-)}] \mu_1 \mu_2 \mu_3 \sigma_0 - \cos[\sqrt{\pi}\Theta_c^{(-)}] \sigma_1 \sigma_2 \sigma_3 \mu_0\}. \tag{13}$$

From the CDWd going through a U(1) QCP one reaches the CDW phase characterized by $(-,-,+)$ and

$$\Theta_c^{(-)} = \sqrt{\pi}/2, \quad \langle \sigma_a \rangle \neq 0 \quad (a = 1,2,3), \quad \mu_0 \neq 0 \tag{14a}$$

or

$$\Theta_c^{(-)} = 0, \quad \langle \mu_a \rangle \neq 0 \quad (a = 1,2,3), \quad \sigma_0 \neq 0. \tag{14b}$$

The order parameter in the continuum limit takes the form

$$\Delta_{CDW} \sim e^{i\sqrt{\pi}\Phi_c^{(+)}} \{\cos[\sqrt{\pi}\Theta_c^{(-)}] \mu_1 \mu_2 \mu_3 \sigma_0 - \sin[\sqrt{\pi}\Theta_c^{(-)}] \sigma_1 \sigma_2 \sigma_3 \mu_0\}. \tag{15}$$

Finally, the SCs phase is dominant in the region $(+,-,-)$ and is characterized by

$$\Theta_c^{(-)} = \sqrt{\pi}/2, \quad \langle \sigma_a \rangle \neq 0 \quad (a = 0,1,2,3) \tag{16a}$$

or

$$\Theta_c^{(-)} = 0, \quad \langle \mu_a \rangle \neq 0 \quad (a = 0,1,2,3). \tag{16b}$$

Its order parameter in the continuum limit is

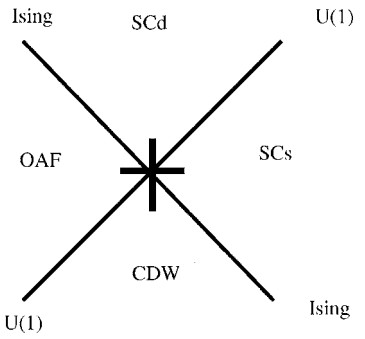

FIG. 1. The two-dimensional projection of the phase diagram for $K_c > 1/2$. The thick lines represent first-order phase transitions. At $K_c < 1/2$ the SC phases are replaced by the Wigner crystal.

$$\Delta_{SCs} \sim e^{i\sqrt{\pi}\Theta_c^{(+)}}\{-i \sin[\sqrt{\pi}\Theta_c^{(-)}]\sigma_1\sigma_2\sigma_3\sigma_0 + \cos[\sqrt{\pi}\Theta_c^{(-)}]\mu_1\mu_2\mu_3\mu_0\}. \quad (17)$$

This last phase can be reached both from the SCd phase through a U(1) QCP or from the CDW phase through a $\mathbb{Z}_2$ critical point. All possible phase transitions are schematically shown in Fig. 1 and can be summarized as follows: $\mathbb{Z}_2$ QCP between SCd and CDWd, SCs and CDW; U(1) QCP between SCd and SCs, CDW and CDWd; and first-order transition between SCs and CDWd, and between SCd and CDW. More details about the phase boundaries are provided in the next section.

The scaling dimension of both CDWs phases is $d_{CDW} = K_c/4$, while the one of SC phases is $d_{SC} = 1/4K_c$. The obtained bosonized expressions for the CDW order parameters differ from the ones obtained in Refs. 14 and 20. In our treatment of the order parameters we used Ising model notations. This is done because Ising model order and disorder parameters σ and μ go naturally with Majorana fermions.

The density operator also contains a $4k_F = 2(k_F^{(+)} + k_F^{(-)})$ oscillatory piece

$$\rho(4k_F;q) = i \exp[i\sqrt{4\pi}\Phi_c^{(+)}][A_q(\chi_R^a\chi_L^a) + B_q\xi_R^3\xi_L^3], \quad (18)$$

where $q = 0, \pi$ is the transverse momentum. Notice that the quasi-long-range order occurs only at the wave vector corresponding to the overall particle density. Correlations with $4k_F^{(+)}, 4k_F^{(-)}$ turn out to be exponentially suppressed. The amplitudes A_Q and B_Q vanish for the noninteracting system, and for weak interactions they are of the order of U/ϵ_F. The importance of the $4k_F$ correlations was pointed out in Refs. 19 and 20. Notice that since the Majorana bilinears always have nonzero expectation values as soon as the spectrum is gapful, the amplitude of the $4k_F$ wave is finite except in the Tomonaga-Luttinger phase and therefore critical $4k_F$ density fluctuations are always present. As a consequence the $4k_F$ order parameter, having the scaling dimension $d_4 = K_c$, competes with the SC ones. At $K_c < 1/2$ the scaling dimension of Eq. (18) becomes smaller than the scaling dimension of the SC order parameters and SC phases on the phase diagram are replaced by the $4k_F$ CDW which we call Wigner crystal.[32] It is possible that this mechanism is responsible for charge ordering in the telephone number compound observed in Refs. 7, 6, and 9. As far as the CDW phases are concerned, the $2k_F$ oscillations are always more relevant. However, an establishment of a true long-range $2k_F$ CDW order in a three-dimensional array of ladders will also lead to condensation of the $4k_F$ oscillations. At special value of $4k_F = 2\pi$ (the 1/4-filled band) operator (18) couples to the lattice. At this point the charge field $\Phi_c^{(+)}$ couples to the other fields and the corresponding sector acquires a gap. As follows from numerical calculations done in Ref. 33, in two-leg ladders this may occur in a broad range of parameters.

As far as the higher harmonics of the electron density with the wave vectors $2nk_F$ are concerned, their scaling dimensions grow as $n^2K_c/4$ and they quickly become irrelevant. For this reason x-ray scattering from such a Wigner crystal shows sinusoidal oscillations of the electron density. This picture holds when the dominant interactions are smaller than the one-dimensional bandwidth so that the continuous description can be used.

The order parameters in the model with weak interchain tunneling (smaller than the gaps) can be obtained from the above order parameters by the chiral particle-hole transformation

$$R_{l,\sigma} \to \sigma R_{l,-\sigma}^{+}. \quad (19)$$

Recall that in the transformed theory l becomes a chain number and Φ and Θ fields in the charge sector interchange.

IV. DISCRETE SYMMETRIES AND PHASE BOUNDARIES

Apart from the continuous symmetries mentioned above, the Hamiltonian (2) possesses a set of discrete symmetries. These symmetries establish a one-to-one correspondence between excitation spectra of the different phases and represent authomorphisms of the O(6) group.[16] To see this we rewrite the interaction (2c) in terms of $SO_1(6)$ Kac-Moody currents $J_a = \psi_R\tau^a\psi_R$ and $\bar{J}_a = \psi_L\tau^a\psi_L$, where $\psi_{R,L}$ represent all six Majorana fermions and τ^a are generators of the O(6) symmetry group

$$V = G_{ab}J_a\bar{J}_b. \quad (20)$$

The discrete transformations which leave the Hamiltonian invariant correspond to a change of sign of some chiral currents and the corresponding coupling constants, leaving the currents of opposite chirality unchanged:

$$J_a \to -J_a, \quad \bar{J}_a \to \bar{J}_a. \quad (21)$$

Since the transformations (21) must preserve the commutation relations of the currents, they correspond to authomorphisms of the corresponding group [the O(6) one in the given case]. The above authomorphisms do not affect the spectrum, but change the order parameters (recall that the latter ones are nonlocal in the Majoranas) and therefore establish a duality between different phases. In terms of Majorana fermions the authomorphisms correspond to a sign change of some Majorana fermions in one chiral sector. Therefore as far as the spectrum is concerned, one can get a complete

picture by studying it in a given phase—for instance, in SCd. All other phases can be obtained using the duality transformations. In the given case we have three dualities

(i) $\xi^3_L \to -\xi^3_L$, $g_{\sigma,-}, g_{c,ss} \to -g_{\sigma,-}, -g_{c,ss}$,
(ii) $\chi^a_L \to -\chi^a_L$, $\xi^3_L \to -\xi^3_L$, $g_{c,st}, g_{c,ss} \to -g_{c,st}, -g_{c,ss}$,
(iii) $\chi^a_L \to -\chi^a_L$, $g_{\sigma,-}, g_{c,st} \to -g_{\sigma,-}, -g_{c,st}$.

Let us now consider in more details the boundaries between the different phases. Since the spectra of different phases are the same, we can take SCd phase as an example.

The boundary corresponding to a $\mathbb{Z}_2$ QCP separating SCd phase from OAF is a surface in the coupling constant space on which the Majorana fermion ξ^3 decouples from the rest and becomes massless. This surface is determined by the condition

$$g_{\sigma,-}\langle(\chi^a_R\chi^a_L)\rangle + g_{c,ss}\langle[(\xi^1_R\xi^1_L) + (\xi^2_R\xi^2_L)]\rangle = 0. \tag{22}$$

The criticality is not violated by fluctuations around Eq. (22) since they cannot generate any relevant operators.

Analogously, if $(\chi^a_R\chi^a_L)$ and $(\xi^3_R\xi^3_L)$ take expectation values and

$$g_{c,st}\langle(\chi^a_R\chi^a_L)\rangle + g_{c,ss}\langle(\xi^3_R\xi^3_L)\rangle = 0, \tag{23}$$

the Majoranas ξ^1, ξ^2 decouple. This is the U(1) QCP between SCd and SCs. The fluctuations generate a perturbation $\cos[\sqrt{16\pi}\beta\Theta^{(-)}_c]$ which may become relevant if $\beta^2 < 1/4$. This, however, corresponds to a very strong $g_{\rho,-}$. Then this critical line may become a first-order transition.

Finally, if

$$g_{\sigma,-}\langle(\xi^3_R\xi^3_L)\rangle + g_{c,st}\langle[(\xi^1_R\xi^1_L) + (\xi^2_R\xi^2_L)]\rangle = 0, \tag{24}$$

with $\langle\xi^a_R\xi^a_L\rangle$ different from zero, the Majorana triplet χ^a is decoupled from ξ fermions. At $g_{\sigma,+} < 0$ both models are massive, which means that this is a first-order transition. The fluctuations shift $g_{\sigma,+}$ further to the negative side. If the effective coupling is positive, however, this becomes a $SU(2)_2$ quantum critical point. The first-order line separates SC and CDW phases with different point-group symmetries (for instance, SCd and CDW).

For the analysis of the spectrum it is convenient to generalize the model (2) to N species of fermions and rewrite the interaction (2c) as

$$V = -\frac{1}{2}X^a\gamma_{ab}X^b, \quad X^a = i\psi^a_R\psi^a_L. \tag{25}$$

The vicinity of the symmetric line of the phase diagram is described by a weakly anisotropic O(N) GN model

$$\gamma_{ab} = \frac{1}{N}(g_0 + \delta g_{ab}), \quad \delta g_{a,b}/g_0 \ll 1. \tag{26}$$

In an analogous way, at the phase boundaries the $N \times N$ matrix γ is split into two $N_1 \times N_1$ and $N_2 \times N_2$ blocks γ^1 and γ^2, respectively,

$$\gamma^0 = \begin{pmatrix} \gamma^1 & 0 \\ 0 & \gamma^2 \end{pmatrix}, \quad \gamma^1_{a,b} = g_1, \quad \gamma^2_{a,b} = g_2, \tag{27}$$

and the vicinity of the phase boundaries is characterized by

$$\gamma_{a,b} = \gamma^0_{a,b} + \delta\tilde{g}_{a,b}, \quad \delta g_{a,b}/g_{1,2} \ll 1. \tag{28}$$

For the case at hand we have $N=6$, and

$$N_1 = 5, \quad N_2 = 1, \quad \text{for } \mathbb{Z}_2, \tag{29}$$

$$N_1 = 4, \quad N_2 = 2, \quad \text{for U(1)}, \tag{30}$$

$$N_1 = 3, \quad N_2 = 3, \quad \text{for the first-order} \tag{31}$$

boundaries, respectively.

V. SEMICLASSICAL ANALYSIS

In this section we provide some general arguments concerning the spectra of generalized O(N) GN models (25)–(28) based on a semiclassical analysis valid in the limit of large N.[27] A more intuitive analysis valid in the same approximation but for even N, M is discussed in Appendix B.

A. Effect of small anisotropy on the vector particles

Let us consider first the generalization (26) of the GN model with a total number of fermion species, N, large. If the quadratic form (25) is negatively defined, then it is possible to perform the Hubbard-Stratonovich transformation introducing an auxiliary field Δ^a,

$$V = \frac{1}{2}\Delta^a(\gamma^{-1})_{ab}\Delta^b - \Delta^a X^a, \tag{32}$$

where Δ is related to X by the equation of motion

$$\Delta^a = \gamma_{ab}X^b. \tag{33}$$

Integrating out the fermions one finds the effective potential for Δ^a,

$$V_{eff}[\Delta] = \frac{1}{2}\Delta^a(\gamma^{-1})_{a,b}\Delta^b + \frac{N}{8\pi}\Delta^2\left(\ln\frac{\Delta^2}{\Lambda^2} - 1\right), \tag{34}$$

which has minima at $\Delta^a = \pm m_a$ given by the saddle point equation

$$m_a = \frac{1}{2\pi}\sum_b \gamma_{ab}m_b \ln(\Lambda/|m_b|). \tag{35}$$

From Eqs. (33) and (34) it follows that the fermion bilinears acquire vacuum expectation values.

Besides the trivial zero-energy solution, the classical static equation of motion for the field Δ in the potential (34) also has finite-energy, kinklike solutions $\Delta_c(x)$ interpolating between different minima (35). When quantizing the theory[31,35] one finds that it possesses fermionic excitations with masses m_a, associated with the ordinary vacuum sector, and kink excitations, associated with configurations $\Delta_c(x)$. In fact, as was shown by Jakiw and Rebbi,[36] fermions interacting with topological kinks like in Eq. (32) possess a single normalizable zero-energy mode ψ_0, in addition to the finite-energy solutions ψ_n. The crucial point is that, while finite-energy solutions are complex, the zero-energy one is real and

nondegenerate. The semiclassical expansion is then given by[36,37]

$$\hat{\psi}^a(x,t) = \hat{\gamma}_a \psi_0^a + \sum_n [\hat{a}_n \psi_n^a(x) e^{-itE_n} + \text{H.c.}], \tag{36}$$

where ψ^0 is the zero-energy solution of the Dirac equation and, assuming that $\Delta_c(+\infty) > 0$, it has the form

$$\psi_0^a = \Omega^{-1/2} \begin{pmatrix} 1 \\ 0 \end{pmatrix} \exp\left[-\int_0^x d\xi \Delta_c^a(\xi) \right], \tag{37}$$

with $\Omega^{-1/2}$ being the normalization factor. Since ψ_a are Majorana fermions, the operators $\hat{\gamma}_a$ compose a Clifford algebra $\{\hat{\gamma}_a, \hat{\gamma}_b\} = \delta_{ab}$. Therefore these matrices realize spinor representations of the O(N) group. It is important to stress that the zero-mode solutions exist for any configuration $\Delta(x)$ which has asymptotics of different sign (a kink). The effect of small anisotropy on the kink masses is difficult to study in the semiclassical limit; this problem will be discussed in Sec. VII C using other methods. We now consider in detail the effect on fermions.

The fermion masses are given by the saddle point equations (35). The solutions of these equations depend on the bare couplings; for $\delta g_{ab} = 0$ one recovers the usual form for the large-N-limit GN mass: namely, $m_a = M_0 = \Lambda e^{-2\pi/g_0}$. If δg_{ab} is nonvanishing but $|\delta g_{ab}|/g_0 \ll 1$, the solution is

$$\frac{\delta m_a}{M_0} = g_0^{-1} \left[\frac{1}{N} \sum_{b \neq a} \delta g_{ab} \right] + g_0^{-2} \left[\frac{1}{N^2} \sum_c \sum_{b \neq c} \delta g_{cb} \right]. \tag{38}$$

From this analysis it is clear that the vector multiplet is split, the splitting being proportional to the splitting of the bare coupling constants, and survives in the limit $1/N \to 0$ provided $N^{-1} \Sigma \, \delta g_{ab} \neq 0$.

Let us now imagine that some of the eigenvalues of γ are zero. The limiting case is when the matrix γ is proportional to the projector:

$$\gamma_{ab} = \frac{1}{N} g e_a e_b, \quad \sum_a e_a^2 = N. \tag{39}$$

Then Eq. (35) can be solved explicitly. The Hubbard-Stratonovich transformation yields

$$\mathcal{L} = \frac{N}{2g} \Delta^2 + \left(\frac{i}{2} \bar{\psi}^a \gamma_\mu \partial_\mu \psi^a - i e_a \Delta \bar{\psi}^a \psi^a \right), \tag{40}$$

and the masses of the vector particles are given by

$$m_a = e_a \langle \Delta \rangle, \tag{41}$$

where

$$\langle \Delta \rangle = \Lambda \exp\left(-\frac{2\pi}{g} + A \right), \quad A = N^{-1} \sum_j e_j^2 \ln(1/|e_j|).$$

The $N \to \infty$ limit is defined as follows:

$$\sum\nolimits_a = N \int de \rho(e), \quad \int de e^2 \rho(e) = 1,$$

$$A = \int de \rho(e) e^2 \ln(1/|e|).$$

So $N-1$ components of vector **e** are RG invariants.

B. Kink confinement

Let us now consider the opposite limit, when two O(N_1) and O(N_2) GN models ($N_{1,2} > 2$) are weakly coupled as in Eqs. (25) and (28). We discuss here only the evolution of the kink excitations since the analysis for the fermions is similar to the one carried out in the previous section.

In the absence of coupling, $\tilde{g}_{ab} = 0$, each GN model has its own kinks, associated with two classical solutions $\Delta_{1,2}(x)$ and interpolating between the minima $\pm m_{1,a}$ and $\pm m_{2,a}$, respectively. The effect of the interaction is to lift the degeneracy between the minima, introducing a confining potential between the kinks. As a consequence the original kink solutions of the decoupled theories become unstable and disappear from the spectrum.

To see this let us consider, for instance, the effect of the interaction on a kink-antikink configuration, where both particles belong to the same GN theory, while the other theory is at the minimum—for example, $\Delta_2(x) = m_2$. The kink-antikink configuration is such that $\Delta_1(x)$ takes the value $-m_1$ from minus spatial infinity to a point $x_1(t)$ where it switches to $+m_1$; it keeps this value until $x_2(t)$ where it switches back to $-m_1$. In the presence of the perturbation, the kink-antikink state acquires an additional energy

$$U(x_1, x_2) = \delta \tilde{g}_{a,b} |x_1 - x_2| m_1 m_2. \tag{42}$$

This results in a confining potential for the two O(N_1) kinks (this universal form of the confining potential is valid only when the confining radius is much greater than the size of the lightest kink). For $N_1 > 4$ this potential exists on top of the attractive potential already present in the O(N_1) GN model. Therefore the lowest bound states have the same symmetry as in the O(N_1) model; i.e., they transform according to the vector representation of the group. Of course, if the confinement radius is much greater than the inverse kink's mass, the confinement potential contains many other bound states (we refer the reader to Sec. VII D for a more detailed analysis). These states do not exist in the O(N_1+N_2) GN model. Their masses are grouped around the mass of the O(N_1) vector particle m_{v1} or, if $N_1 \leqslant 4$, around $2M_1$, where M_1 is the kink's mass in the O(N_1) GN model. Repeating the same argument for a kink-antikink configuration belonging to the O(N_2) GM model one obtains the states grouped around the mass of the O(N_2) vector particle m_{v2}.

The same confining phenomenon happens also between two kinks that belong to different GN models; in this case the lowest multiplet of the confined states transforms according to the spinor representation of O(N_1+N_2). This follows from the fact that such states correspond to a simultaneous change of sign of $\Delta_1(x)$ and $\Delta_2(x)$; therefore they are kinks of the O(N_1+N_2) GN model. Since the only interaction between kinks of the different models is proportional to $\delta \tilde{g}_{a,b}$, the masses of these particles group around the sum of the

kinks masses M_1+M_2. The details of the structure of the excitations induced by the confining potential is discussed in Sec. VII. One should keep in mind that some multiple kink representations may survive (see Appendix B).

C. Coupling massless and massive GN models

The above analysis fails if the matrix γ in Eq. (25) has negative eigenvalues. If all eigenvalues are negative, the analysis of the RG equations shows that all interactions scale to zero, leaving the theory massless. The situation when the form has no definite sign (at least, this is the criterion in the large-N limit) corresponds to the area of the emergent attraction. The large-N analysis is still applicable here, but in a modified form. Let us consider the $\mathrm{O}(N_1)\times\mathrm{O}(N_2)$ model with N_1/N_2 finite in a situation such that the interaction among the first N_1 particles is attractive and the interaction among the other particles is repulsive. We take a simple form of the interaction to keep the analysis more clear. Then we can do the Hubbard-Stratonovich transformation in the attractive sector, so that after some algebraic manipulations we obtain $(g_+, g_- > 0)$

$$
\begin{aligned}
&-\frac{g_+}{N_1}(\mathrm{i}\bar{\xi}_a\xi_a)^2+2\frac{g_X}{N_1}(\mathrm{i}\bar{\xi}_a\xi_a)(\mathrm{i}\bar{\chi}_b\chi_b)+\frac{g_-}{N_1}(\mathrm{i}\bar{\chi}_b\chi_b)^2\\
&\quad\to\frac{N_1}{2g_+}\Delta^2+\mathrm{i}\Delta\left(\bar{\xi}_a\xi_a-\frac{g_X}{g_+}\bar{\chi}_b\chi_b\right)\\
&\quad\quad+N_1^{-1}\left(\frac{g_X^2}{g_+}+g_-\right)(\mathrm{i}\bar{\chi}_b\chi_b)^2. \qquad (43)
\end{aligned}
$$

Replacing Δ with a constant $M_0\approx m_\xi/g_+$ where m_ξ is a mass of ξ fermions, we obtain the following Lagrangian for χ fermions:

$$
\mathcal{L}=\frac{\mathrm{i}}{2}\bar{\chi}_a\gamma_\mu\partial_\mu\chi_a+\mathrm{i}M_0\bar{\chi}_a\chi_a-g_{\mathrm{eff}}(\bar{\chi}_a\chi_a)^2, \qquad (44)
$$

where $g_{eff}=N_1^{-1}(g_X^2/g_++g_-)$. Summing the diagrams with a maximal number of loops, we obtain the following expression for the mass ratio:

$$
\frac{m_\chi}{m_\xi}=-\frac{g_X}{g_+}\left[1+\frac{N_2}{N_1}(g_X^2/g_+^2+g_-/g_+)\right]^{-1}. \qquad (45)
$$

Thus also in this case the vector multiplet remains split.

Let us now consider kinks. When one of the GN models is massless the potential (42) can no longer be used. Like above, we can do the Hubbard-Stratonovich transformation in the massive sector [cf. Eq. (43)] and study the problem of the two types of fermions in a background bosonic field. For both fermionic modes the solution is again described by Eqs. (36) and (37). As was discussed in Sec. V A, the entire kink is a bound state of the scalar field $\Delta(x)$ and the fermions. The fermionic zero modes now realize spinor representations of the $\mathrm{O}(N_1+N_2)$ group and then in principle can be seen as bound states of massive kinks of the $\mathrm{O}(N_1)$ model and massless one of the $\mathrm{O}(N_2)$.

The summary of these semiclassical arguments is the following. Weak interactions between GN models generate (i) degenerate kink multiplets transforming according to spinor representations of the $\mathrm{O}(N_1+N_2)$ groups and (ii) vector particles with different masses transforming according to the vector representations of the $\mathrm{O}(N_1)$ and $\mathrm{O}(N_2)$ groups. On top of it there may be many other multiplets with masses lying between (M_1+M_2), m_{v1}, m_{v2}, and $2(M_1+M_2)$. These multiplets cross into the continuum and become progressively unstable once the coupling between two models increases.

VI. INTEGRABLE POINTS

At some specific points in the parameter space the Hamiltonian (2) is integrable. One can identify the following integrable models, which describe either the most symmetric points or the phase boundaries.

O(6) GN *model*. As already noticed, if all coupling constants are equal, Eq. (2) has an extended O(6) symmetry and becomes the O(6)-symmetric GN model (4). The O(N) GN model is integrable for any N.[34,38,39] For even N the scattering theory is relatively simple,[40] while for N odd there are significant complications (see Ref. 41). For $g<0$ and $N>2$ the spectrum is massive and consists of kinks and antikinks, which transform according to the irreducible spinor representations of the O(N) group. For N even kinks and antikinks correspond to different representations; for N odd there is just one representation. The two-loop RG gives the following expression for the mass:

$$
M=\Lambda g^{1/(N-2)}\exp[-2\pi/(N-2)g]. \qquad (46)
$$

For $N>4$, there are also fermion particles and their bound states. These fermions correspond to the original Majorana fermions and transform according to the vector representation of the group. The masses of the fermions and their bound states are given by

$$
M_a=2M\sin\left(\frac{\pi a}{N-2}\right),\quad a=1,\ldots,\mathrm{int}\left(\frac{N-3}{2}\right). \qquad (47)
$$

For N even, the total number of kinks is $2^{N/2}$ [reflecting the fact that there are two $2^{N/2-1}$-dimensional irreducible spinor representations of the algebra SO(N) (Ref. 37)]. For N odd, the total number of kinks is $2^{(N+1)/2}$ although there are major subtleties associated with multiparticle states.[41] The number of fermions is always N. In particular, for $N=6$ the spectrum consists of two spinor multiplets of mass M and one sixfold-degenerate vector multiplet with mass $\sqrt{2}M$. No fermion bound states are present. An intuitive picture of the two types of excitations is provided in Appendix B for N even. It is also good to remember that the spinor representations of O(6) are isomorphic to fundamental representations of the SU(4) group; their quantum numbers correspond to spin $\sigma=\pm 1/2$ and transverse momentum $p=0,\pi$ (or chain index for theories with weak interchain tunneling).

$\mathrm{O}(3)\times[\mathrm{U}(1)\times\mathbb{Z}_2]$ *model*. For $g_{\sigma-}=g_{c,st}=0$ two groups of Majoranas decouple from each other; one is described by the O(3) GN model, the other one by the anisotropic O(3) GN $[\mathrm{U}(1)\times\mathbb{Z}_2$ symmetric]. Both models are integrable (see Refs. 45 and 46), and the excitation spectrum contains only kinks.

(3+1) *model*. At the U(1) QCP, described earlier in Sec. III, two Majorana fermions $\xi_{1,2}$ decouple and remain massless. The remaining massive theory with the $O(3)\times\mathbb{Z}_2$ symmetry is related to an integrable model solved by Tsvelik[42] and Andrei and Jerez.[43] (Some correlation functions for this model were calculated in Ref. 44.) The spectrum of this integrable model contains an SU(2) kink doublet with mass M and a light Majorana fermion of mass $m_0 \sim M(\lambda - \lambda')$. There are no stable vector particles except for this singlet fermion, which is, however, *not* a bound state of kinks (see the discussion at the end of the next paragraph). The S-matrix can be found in Appendix C.

(5+1) *model*. At the Ising QCP one Majorana decouples. For $g_{\sigma,+}=g_{\rho,-}=g_{c,st}$ the massive model is O(5) symmetric and integrable. Outside of the QCP, provided the O(5) symmetry is maintained ($g_{c,ss}=g_{\sigma,-}$), it is possible to construct a factorized scattering (integrable) theory with the same symmetry, $O(5)\times\mathbb{Z}_2$, and UV central charge. The exact solution is described in Appendix C; the spectrum consists of two vector particles (quintet and singlet of Majorana fermions) with different masses m_0 and $\sqrt{3}M$ and a quartet of kinks $\equiv$antikinks with mass M realizing the spinor representation of the O(5) group. This theory certainly deserves further analysis. There are two serious qualitative differences between the scattering theories for the (5+1) model and the O(6) GN model [similar differences are found between the (3−1) model above and the O(4)]. First, as follows from group theory, in the former case the kinks and antikinks are the same particles and in the latter case they belong to different representations. Second, in the (5+1) theory the singlet fermion does not appear as a bound state of kinks as all vector particles do in the O(6) GN model. As a consequence the singlet mass is not related to the kink's mass. One would imagine, however, that with an increase of the coupling between the Majorana singlet and the other ones the model approaches the O(6) GN model. At present we do not have a complete picture of reconciliation of these two models. The most likely solution to this puzzle is that the two theories are equivalent only in the region where the singlet mass is small.

VII. PERTURBING AROUND INTEGRABLE POINTS

In this section we discuss how to calculate the spectrum using perturbation theory around integrable points. Since integrable points describe the phase boundaries and highly symmetric points, we will be able to obtain some additional information about the excitations of the model in these regions.

A. Form-factor perturbation theory

Let us first recall some essential features of integrable models that we need in order to construct perturbation theory. Massive integrable models are characterized by a simplified on-shell dynamics which is encoded into a set of elastic and factorized scattering amplitudes of their massive particles. A convenient formalism for the description of a dilute gas of particles with factorized scattering can be constructed in terms of the creation and annihilation operators $A_a^\dagger(\theta)$ and $A_a(\theta)$, which satisfy the Zamolodchikov-Faddeev (ZF) algebra. (For an introduction to these concepts see, for instance, Refs. 30 and 38 or the introductory chapters of Smirnov's book in Ref. 47.) Here the rapidity θ parametrizes the relativistic dispersion relation

$$e_a(\theta) = M_a \cosh\theta, \quad p_a(\theta) = M_a \sinh\theta \tag{48}$$

and a is an isotopic index. The ZF operators are the logical extension of the algebra of free fermions or bosons to the case of interacting particles with factorizable scattering, where the interaction is completely characterized by the two-particle S-matrix $S_{a,b}(\theta_{ij})$.[38] As usual, multiparticle states are obtained acting with strings of creating operators on the vacuum:

$$|\theta_1, \ldots, \theta_n\rangle_{a_1,\ldots,a_n} = A_{a_1}^\dagger(\theta_1)\cdots A_{a_n}^\dagger(\theta_n)|0\rangle. \tag{49}$$

The single-particle states can be thought as generated by an operator $\varphi_a(x)$ such that $\langle 0|\varphi_a|\theta\rangle_a \neq 0$. For the O($N$) GN model ZF operators include fermion, A_{f_i} (and their bound states), and kink, A_{k_i}, operators. Though for the O(N) GN model the S-matrix is not diagonal, this will not be essential for what follows, so we prefer to describe the methods for diagonal S-matrices since the notations are less cumbersome.

In what follows we will need a definition of nonlocality. Recall that two operators $\mathcal{O}_1$ and $\mathcal{O}_2$ are said to be mutually nonlocal if the Euclidean correlator $\langle\cdots\mathcal{O}_1(x)\mathcal{O}_2(0)\cdots\rangle$ is not a single-valued function of x. In particular, if we introduce the complex variables $z=x^1+ix^2$ and $\bar{z}=x^1-ix^2$, and under analytic continuation $z\to ze^{2\pi i}$, $\bar{z}\to\bar{z}e^{-2\pi i}$, the correlator acquires only a phase $2\pi\gamma_{1,2}$, the two operators are said to be *semilocal*. The nonlocal operators that we will consider in the following are of this type. The great usefulness of this definition is that the index $\gamma_{1,2}$ can be calculated in the ultraviolet, where all correlation functions have a simple power-law form. As we will see, the effect of a perturbation on the spectrum of a theory will crucially depend on the locality properties of the perturbing operator.

Let us imagine now that we perturb an integrable theory H_{int} with a nonintegrable perturbation

$$H = H_{int} - g\int \mathrm{d}x\Psi(x), \tag{50}$$

where $\Psi(x)$ is a scalar field. The variation of the spectrum of the theory can be studied perturbatively in g, in the same spirit as standard quantum mechanics (QM) perturbation theory, taking advantage of the fact that in integrable models matrix elements of perturbing operators

$$F^{\Psi}_{b_1,\ldots,b_m;a_1,\ldots,a_n}(\theta'_1,\ldots,\theta'_m;\theta_1,\ldots,\theta_n) = {}_{b_1,\ldots,b_m}\langle\theta'_1,\ldots,\theta'_m|\Psi(0)|\theta_1,\ldots,\theta_n\rangle_{a_1,\ldots,a_n}, \tag{51}$$

or form factors (FF's), can be computed exactly.[47] The related perturbative approach is called form-factor perturbation theory (FFPT).[28]

According to Ref. 28, the first-order term in the expansion of the mass variation of the particle A_a is given by

$$\delta m_a^2 \simeq 2g_a \langle\theta|\Psi(0)|\theta\rangle_a = 2gC^{a,a'}F^{\Psi}_{a',a}(i\pi), \tag{52}$$

where the two-particle FF $F^{\Psi}_{a_1,a_2}(\theta_1-\theta_2) = \langle 0|\Psi(0)|\theta_1,\theta_2\rangle_{a_1,a_2}$ depends on the difference of the rapidities only if Ψ is a scalar operator. In Eq. (52) we used the crossing property valid for Lorentz scalars,

$$F^{\Psi}_{b_1,\ldots,b_m;a_1,\ldots,a_n}(\theta_1',\ldots,\theta_m';\theta_1,\ldots,\theta_n) = \prod_{j=1}^{m} C^{b_j,b_j'} F^{\Psi}_{b_1',\ldots,b_m',a_1,\ldots,a_n}(\hat{\theta}_1',\ldots,\hat{\theta}_m',\theta_1,\ldots,\theta_n), \tag{53}$$

where $\hat{\theta}=\theta+i\pi$ and C is the charge conjugation matrix satisfying two requirements: $C^t=C$ and $C^2=I$. For Majorana fermions C is trivial because they are neutral.

Since this is a strong-coupling (IR) analysis, if g in Eq. (50) scales under RG, it has to be replaced in Eq. (52) by its renormalized value at energy of the order of the largest mass in the theory:

$$g \to g^{eff} \simeq g(m). \tag{54}$$

The definition of the coupling constant at energy m is somewhat ambiguous. The problem is that RG equations are universal only in the first loop and beyond this they depend on the regularization scheme. By introducing g^{eff} we stretch these equations to their limit. Therefore we will not be able to establish a rigorous relationship between the IR and UV parameters.

In analogy with QM degenerate perturbation theory, the perturbed masses for degenerate multiplets are obtained by diagonalizing the matrix $\{M_{m,n}\}=\{F^{\Psi}_{n,m}(i\pi)\}$, where the indices n and m belong to the degenerate multiplet. If the symmetry of the perturbing operator is less than the symmetry of the multiplet, the perturbation will split it.

Assuming that the IR coupling constants in Eq. (52) are smooth functions of the bare ones and $F^{\Psi}(i\pi)_{\bar{a},a}$ is finite, the spectrum evolves adiabatically. However, there are effects which do not appear in the first order. The perturbation may also generate an effective attraction between the particles and lead to an enlargement of the particle content of the theory through the formation of bound states below the two-particle threshold. For small g^{eff} the appearance of bound states can be studied solving the eigenvalue equation for the two-particle wave function. This will be done in some detail later in the text [cf. Eq. (64)].

A more dramatic change in the particle content of the theory happens when Ψ is nonlocal with respect to the operator φ_a, which generates the particle a.[28] In this case, as shown below, the two-particle FF $F^{\Psi}_{\bar{a},a}(\theta)$ has a pole for $\theta=i\pi$ and then the mass variation (52) diverges. This infinite mass variation implies that the original particle a (it will be called a "quark" in analogy with high-energy physics) is confined and disappears from the spectrum of the perturbed theory. The resulting spectrum consists of quark bound states—"mesons." Their masses may be higher than the two-quark threshold. The analysis of the meson spectrum will be done in Sec. VII D.

The way the nonlocality properties of an operator affect its FF's can be seen as follows. From the general theory of FF's it is known that the n-particle FF has kinematical poles, associated with annihilation processes, whenever the rapidities of a particle and antiparticle differ by $i\pi$. The residue is given by[47]

$$-i\mathrm{Res}_{\theta'=\theta}F^{\Psi}_{\bar{a},a,a_1,\ldots,a_n}(\theta'+i\pi,\theta,\theta_1,\ldots,\theta_n) = \left(1-e^{2\pi i\gamma_{a,\Psi}}\prod_{i=1}^{n}S_{a,a_i}(\theta-\theta_i)\right)F^{\Psi}_{a_1,\ldots,a_n}(\theta_1,\ldots,\theta_n), \tag{55}$$

where $\gamma_{a,\Psi}$ is the semilocality index between φ_a and Ψ. It is easy to see that for two particles ($n=0$) the right-hand side (RHS) vanishes if $\gamma_{a,\Psi}$ is an integer. Then a two-particle FF has a pole at $\theta=i\pi$ only if the operator is nonlocal. As a consequence of Eq. (55) the mass variation (52) induced by a nonlocal operator is infinite. From Eq. (55) it follows that for $(\theta\sim\theta')$

$$F^{\Psi}_{\bar{a},b,a',b'}(\theta+i\pi,-\theta+i\pi,\theta',-\theta') \simeq -\alpha_{a,b}\langle\Psi\rangle\left[\frac{\delta_{a,a'}\delta_{b,b'}}{(\theta-\theta')^2}+\frac{\delta_{a,b'}\delta_{b,a'}}{(\theta+\theta')^2}S_{a,b}(2\theta')\right], \tag{56}$$

with $\alpha_{a,b}=(1-e^{2i\pi\gamma_{a,\Psi}})(1-e^{2i\pi\gamma_{b,\Psi}})$. This will be needed in the following.

The factorized scattering approach can also be constructed for massless integrable models,[48] despite the subtleties in defining a scattering theory between massless particles in 1+1 dimensions. In this case the excitations are right- and left-moving particles $A_R(\theta)$, $A_L(\theta)$ with dispersion relation $e_R(\theta)=p_R(\theta)=(M/2)e^{\theta}$ and $e_L(\theta)=-p_L(\theta)=(M/2)e^{-\theta}$, where M here is just a scale (for simplicity we consider only particles with no internal indices; this is the only situation that we will encounter in the following). Also the FF's can be defined and computed in analogy with the massive case,[49] and FFPT can be used to study the mass generation, which, to first order, will be given by[50]

$$\delta m \simeq gF^{\Psi}_{R,L}(i\pi-\infty), \tag{57}$$

where $F^{\Psi}_{R,L}(\theta)$ is the right-left FF:

$$F^{\Psi}_{R,L}(\theta_{12}) = \langle 0|\Psi(0)|A_R^{\dagger}(\theta_1)A_L^{\dagger}(\theta_2)\rangle. \tag{58}$$

Also in this case confinement is related to the nonlocality properties of the perturbing operator.[50]

B. Nonlocality properties of the perturbing operators

In order to apply the above methods to deformations of GN models like in Eqs. (25)–(28), let us study the locality properties of the perturbing operators with respect to the GN particles.

Consider first a massive O(N) GN model ($N>2$). Generally speaking an operator of the form $\Psi_1=\psi_R^a\psi_L^a$ is local with respect to the vector particles A_{f_i}, but not with respect to the kinks A_{k_i}. This can be easily seen even without explicitly

introducing kink creating operators. In fact the kink is an elementary excitation of the GN model that interpolates between positive and negative minima of $\psi_R^a\psi_L^a$ and therefore this operator changes sign across a kink configuration. This implies that the nonlocality index between the kink creating operator and Ψ_1 is $e^{2i\pi\gamma}=-1$, but at the same time, an operator that is a product of two fermionic bilinears belonging to the same GN model, $\Psi_2=\psi_R^a\psi_L^a\psi_R^b\psi_L^b$, is local also with respect to the kinks. As a consequence, Eq. (52) can be safely used to evaluate the first-order effect of deforming the O(N) GN according to Eq. (26), since the perturbation is local with respect to both kinks and fermions. This implies that the spectrum will evolve adiabatically; the only important effect is to split the degeneracy between some states as discussed in the next section.

On the other hand, if one takes two different massive GN models—say, $H_{O(N)}[\chi]$ and $H_{O(M)}[\xi]$ $(N,M>2)$—and couples them like in Eq. (28), the perturbation $\Psi_3=\chi_R^a\chi_L^a\xi_R^b\xi_L^b$ is nonlocal with respect to the kinks of the two GN models, thus leading to their confinement. This is in agreement with the semiclassical analysis of Sec. V.

C. First-order effects: Perturbations around the O(6)-symmetric point

We first apply FFPT to study the spectrum of vector particles around the O(6)-symmetric point. We consider small deviations of coupling constants in Eqs. (2) from the point where all of them are equal, $g_a=g+\delta g_a$ $(a=[\rho,-],[c,ss],[\sigma,-],[c,st],[\sigma,+])$. The perturbation is local and then Eq. (52) can be safely applied, with g_a replaced by $g_a(m)$. It should be emphasized that the coupling constants g_a carry information about physical quantities only when they are small. Beyond the first-loop approximation RG equations are not universal depending on the regularization scheme. We assume that the interaction between physical particles does not change substantially once $g_a\sim 1$ and therefore stretching the RG equations to the limit of their validity, $\ln(\epsilon/m)\sim 1$, we can estimate the anisotropy of the coupling constants in the strong-coupling regime. This assumption is not justified but its consistency with know results will be checked.

For $\delta g_a/g\ll 1$ we can linearize the RG equations (5). The details of the calculations with all notations are given in Appendix D. We find

$$\delta g_a(\varepsilon)=A_0[\ln(\varepsilon/m)]^{-2}+(T_{a,1}C_{-1/2,+}+T_{a,2}C_{-1/2,-})\times[\ln(\varepsilon/m)]^{1/2}+(T_{a,3}C_{1/2,+}+T_{a,4}C_{1/2,-})\times[\ln(\varepsilon/m)]^{-1/2}, \tag{59}$$

where $C_{q,\pm}\sim\delta_q g(0)g_0^{-q}$ (δ_q stands for a particular linear combination of couplings) are RG invariants, which can be obtained explicitly using the results of Appendix D, and $A_0\sim\Sigma\delta g_a(0)/g_0^2$. At scales of the order of the mass we can set $\ln(\varepsilon/m)\approx 1$ in Eq. (59) and substitute the result into Eq. (52). By dimensionality considerations the matrix element of the current-current product is const$\times m^2$. We remark that this normalization yields the correct estimate of the mass change at the uniform variation of the coupling constants. Indeed, in this case, according to Eq. (59), the change of the effective coupling at energy m is $\delta g_0/g_0^2$ and Eq. (52) gives $\delta m\sim\delta g_0/g_0^2 m$. On the other hand, we obtain the same estimate from the known dependence of the mass on the bare coupling:

$$\delta m^2=\frac{\partial m^2}{\partial g_0}\delta g_0=-\frac{2m^2\pi}{g_0^2}\delta g_0. \tag{60}$$

It is interesting to estimate the mass splittings for the case of small g_0. Then the largest RG invariants that produce a splitting of the multiplet are $C_{1/2}$ (the most relevant term, proportional to A_0, is the same for any fermion). Taking only them into account we obtain the following mass corrections:

$$\frac{\delta m_c^{(-)}}{m}\sim[\delta g_{\rho,-}(m)+\delta g_{c,ss}(m)+3\delta g_{c,st}(m)]\sim C_{1/2,+}+C_{1/2,-},$$

$$\frac{\delta m_s^{(s)}}{m}\sim[3\delta g_{\sigma,-}(m)+2\delta g_{c,ss}(m)]\sim C_{1/2,+}-2C_{1/2,-},$$

$$\frac{\delta m_s^{(tr)}}{m}\sim[2\delta g_{\sigma,+}(m)+\delta g_{\sigma,-}(m)+2\delta g_{c,st}(m)]\sim -C_{1/2,+}. \tag{61}$$

One can conclude from Eq. (61) that for any finite RG invariants the O(6) vector multiplet is split. Nevertheless, the splitting is very small in the regime of validity of this analysis.

Let us now apply Eq. (52) to study the evolution of the kink masses. Since they are degenerate, we need to diagonalize the matrix with elements $k_i\langle\theta_i|\psi_R^a\psi_L^a\psi_R^b\psi_L^b|\theta_j\rangle_{k_j}$, where $k_{i,j}$ indicate kinks of the degenerate multiplet. The needed FF has the form[51]

$$F_{k_i,k_j}^{a,b}(\theta_{ij})=\langle 0|\psi_R^a\psi_L^a\psi_R^b\psi_L^b|\theta_i,\theta_j\rangle_{k_i,k_j}=(1-\delta_{a,b})C_{k_i,k_j}f(\theta), \tag{62}$$

where C is the charge conjugation matrix and the function $f(\theta)$ is finite at $\theta=i\pi$. From this, using Eq. (53), one gets that, for $a\neq b$,

$$_{k_i}\langle\theta_i|\psi_R^a\psi_L^a\psi_R^b\psi_L^b|\theta_j\rangle_{k_j}=\delta_{k_i,k_j}f(\theta), \tag{63}$$

and then the matrix is diagonal. Using now Eq. (52) one finds that the mass variation is the same for any kink and then the multiplet is not split.

D. Beyond the first order

Let us now turn to the problem of kink confinement induced by a nonlocal operator. This analysis in important to study the spectrum close to the first-order transition line. In this case the FF in Eq. (52) is infinite and this formula cannot applied. Nevertheless, for g^{eff} sufficiently small the lower part of the meson spectrum can be studied within the two-quarks approximation described in Ref. 52 in the context of the Ising model. It is convenient to parametrize the ZF operators directly in terms of momentum; the relationship be-

tween the two parametrizations can be found in Eq. (48). The two-particle wave function can be written in the center-of-mass frame as

$$|\Psi_{a,b}\rangle = \int_{-\infty}^{+\infty} \mathrm{d}\tilde{\psi}_{a,b}(p) A_a^\dagger(p) A_b^\dagger(-p)|0\rangle. \tag{64}$$

In general a and b can be different particles with masses M_a and M_b, but both nonlocal with respect to Ψ. Note that the wave function is not written in an explicit relativistic invariant form although the states have a relativistic normalization. The eigenvalue problem gives the equation

$$[E - e_a(p) - e_b(p)](\tilde{\psi}_{a,b}(p)\delta_{a,a'}\delta_{b,b'} + \tilde{\psi}_{b,a}(p)\delta_{a,b'}\delta_{b,a'}) = g^{eff}\int_{-\infty}^{\infty} \mathrm{d}p'\, {}_{a,b}\langle p,-p|\Psi(0)|p',-p'\rangle_{a',b'}\tilde{\psi}_{a',b'}(p'), \tag{65}$$

where g^{eff} is the renormalized coupling constant at energy $\sim(M_a+M_b)$. For energies close to the threshold (small momentum) one can approximate $E-e_a(p)-e_b(p) \simeq \epsilon - p^2/2\mu$, with $\epsilon = E-(M_a+M_b)$ and $\mu = M_a M_b/(M_a+M_b)$. If the operator is nonlocal, it follows from Eq. (55) that the right-hand side is dominated by the double pole in the four-particle FF. It will be convenient for us to distinguish between two cases. One is the confinement of identical particles, and the other is when confining particles are not identical having, in general, different masses. These two cases are qualitatively similar, but there are differences in details.

We consider first the confinement of two kinks that belong to different GN models induced by the operator $\Psi_3 = \chi_R^a \chi_L^a \xi_R^b \xi_L^b$. Let us call a_i kinks that belong to $H_{O(N)}[\chi]$ and b_i kinks that belong to $H_{O(M)}[\xi]$. Given the structure of the potential, the FF factorizes as

$$ {}_{a_1,b_1}\langle p_1,p_2|\Psi_3|p_1',p_2'\rangle_{a_2,b_2} = {}_{a_1}\langle p_1|(\chi_R^a\chi_L^a)|p_1'\rangle_{a_2} {}_{b_1}\langle p_2|(\xi_R^b\xi_L^b)|p_2'\rangle_{b_2}. \tag{66}$$

According to Eqs. (55) and (56) for $p \sim p'$ we can approximate

$$ {}_{a_1}\langle p_1|(\chi_R\chi_L)|p_1'\rangle_{a_2} \simeq \frac{2\mathrm{i}M_a}{(p_1-p_1')}\langle\chi_R\chi_L\rangle\delta_{a_1,a_2}, \tag{67}$$

where we have used the fact that $\mathrm{e}^{2\mathrm{i}\pi\gamma_{a,\Psi_3}} = -1$. Clearly the same approximation is valid for ${}_{b_1}\langle p_2|(\xi_R\xi_L)|p_2'\rangle_{b_2}$. From this we get the eigenvalue equation

$$(-\epsilon + p^2/2\mu)\tilde{\psi}_{a,b}(p) = \lambda_{a,b}\mathcal{P}\int_{-\infty}^{\infty}\frac{\mathrm{d}p'}{(p-p')^2}\tilde{\psi}_{a,b}(p'), \tag{68}$$

where $\mathcal{P}$ indicates the principal part and

$$\lambda_{a,b} = 4g_{a,b}^{eff}\langle\chi_R\chi_L\rangle\langle\xi_R\xi_L\rangle M_a M_b. \tag{69}$$

After a Fourier transform to configuration space Eq. (68) takes the form

$$\left(-\epsilon + \lambda_{a,b}|X| - \frac{1}{2\mu}\frac{\mathrm{d}^2}{\mathrm{d}X^2}\right)\tilde{\psi}_{a,b}(X) = 0, \tag{70}$$

where

$$\tilde{\psi}_{a,b}(X) = \int \frac{\mathrm{d}p}{2\pi}\mathrm{e}^{\mathrm{i}pX}\tilde{\psi}_{a,b}(p). \tag{71}$$

In general this equation must be supplemented by symmetry conditions.

The eigenvalue equation (71) describes a particle confined in a linear potential. The solution is well known.[53] In the region $X>0$ one can introduce the new variable $\zeta = (2\lambda_{a,b}\mu)^{1/3}(X - \epsilon/\lambda_{a,b})$ so as to yield

$$\left(\frac{\mathrm{d}^2}{\mathrm{d}\zeta^2} - \zeta\right)\Psi(\zeta) = 0 \tag{72}$$

at $\zeta > -(2\mu/\lambda_{a,b}^2)^{1/3}\epsilon$, from which it follows that the solution is the Airy function

$$\tilde{\psi}_{a,b}(\zeta) \propto \mathrm{Ai}(\zeta). \tag{73}$$

The eigenstates are determined either by the zeros of the derivative of the Airy function $\mathrm{Ai}'(\zeta)$ at $X=0$ (symmetric wave functions) or by the zeros of the function itself (antisymmetric wave functions). Calling them ζ_i we have

$$E_i - (M_a+M_b) = (\lambda_{a,b}^2/\mu)^{1/3}\zeta_i$$

$$[\mathrm{Ai}'(-\zeta_i) = 0 \text{ or } \mathrm{Ai}(-\zeta_i) = 0]. \tag{74}$$

Clearly, if the particles a, b are identical, the above analysis requires minor modifications as we will see below.

In agreement with the semiclassical arguments of Sec. IV we see that the kinks of the $\mathrm{O}(N_1)$ and $\mathrm{O}(N_2)$ models disappear from the spectrum and are replaced by the generations of mesons which energies belong to the original two-particle continuum starting from M_1+M_2. Stable meson states must have spectral gaps smaller than $E_i < 2E_1 \approx 2(M_1+M_2)$. The above analysis is quantitatively valid if the number of meson generations is large. For the simplified model $\mathrm{O}(3)\times\mathrm{O}(3)$ it is easy to express this number in terms of the RG invariants. Setting $\Delta_{1,2} = \mathrm{const}\times M_{1,2}$ we find from Eqs. (89) below that at $g_+ \sim -1$ the effective coupling constant is

$$g^{eff} \sim [2|C_{1/2}| + C_{-1/2}]^{-2} \tag{75}$$

provided $|C_{1/2}| + C_{-1/2} \gg 1$. Then using Eq. (69) we obtain

$$(g_{ab}^2/\mu)^{1/3} \sim (M_1+M_2)\left[g^{eff}\frac{\sqrt{M_1M_2}}{M_1+M_2}\right]^{2/3}. \tag{76}$$

Since $\zeta_i \sim i^{2/3}$ at $i \gg 1$, this sets the limit for the number of meson generations as

$$i_{max} \sim g_{eff}^{-1}(\sqrt{M_1/M_2} + \sqrt{M_2/M_1}). \tag{77}$$

Thus it appears that the limit of weak confinement can be achieved by either taking small g_{eff} or considering quarks with vastly different masses. These two routes, however, lead to nonequivalent limits. The limit $M_1/M_2 \to 0$ is different from the limit $g_{eff} \to 0$ and cannot be studied using the above

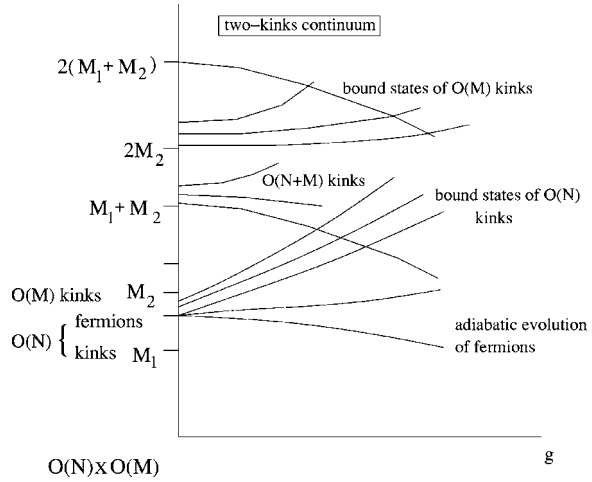

FIG. 2. A qualitative picture of the spectrum of the O(N) $\times$O(M) GN model.

formulas. The reason is that when the confinement radius $(g_{eff}M_1M_2\mu)^{-1/3}$ becomes of the order of the size of the lightest kink M_1^{-1}, one can no longer use Eq. (67). Thus the above analysis is valid only at

$$M_1 \gg g_{eff}M_2. \tag{78}$$

At smaller mass ratios one can either use more accurate expressions for the FF's or resort to the semiclassical analysis of Sec. V B. As we know from this analysis, confinement of a light particle on a heavy kink produces a zero-energy bound state and the scattering continuum separated from the bound state by a gap of the order of $g_{eff}M_2$. This is of the order of the energy of the lowest bound state $(g_{ab}^2/\mu)^{1/3}$ at $M_1 \sim g_{eff}M_2$.

Let us repeat the above analysis for confinement of identical particles ($M_a=M_b=M$) induced, for instance, by an operator Ψ. As we discussed in Sec. IV, this leads to the formation of vector particles. Within the integral of Eq. (65), we can approximate

$$_{a,b}\langle p,-p|\Psi(0)|p',-p'\rangle_{a',b'} \simeq -M^2\langle\Psi\rangle\left[\frac{\delta_{a,a'}\delta_{b,b'}}{(p-p')^2}-\frac{\delta_{a,b'}\delta_{b,a'}}{(p+p')^2}\right]. \tag{79}$$

With a few manipulations Eq. (65) can be put into the form (79) with $\lambda_{a,b}=4g^{eff}M^2\langle\Psi\rangle$. In this case the particles are indistinguishable, so only antisymmetric Airy functions are acceptable. The summary of the above results is shown schematically in Fig. 2.

It should also be noticed that if the unperturbed theory, like in the case of the O(N) GN model, possesses bound states of mass $M_{a,b}$ between particles a and b (associated with poles of the S-matrix on the physical strip), the eigenvalue equation (65) has to be modified taking into account this residual attraction,

$$[E-e_1(\theta)-e_2(\theta)] \to [E-e_1(\theta)-e_2(\theta)+\Delta E_{a,b}], \tag{80}$$

where $\Delta E_{a,b}=M_1+M_2-M_{a,b}$. As a consequence, Eq. (70) is modified as

$$\left(-\epsilon-\frac{1}{2\mu}\frac{d^2}{dX^2}+\lambda|X|-b_0\delta(X)\right)\psi_{\alpha,\beta}(X)=0. \tag{81}$$

The δ function is chosen in such a way that vector particles appear also at $\lambda=0$. For the O(3) case, $b_0=0$.

The formation of bound states induced by a local perturbation can be discussed in similar terms. For small g^{eff} the two-particle wave function can be taken in the form (64) from which the eigenvalue equation (65) follows. The crucial difference with respect to the case discussed above is that, since the, operator is local, the four-particle FF's in Eq. (65) only have first-order, poles giving rise to a nonsingular potential. Bound states form if the perturbation is such that there is a solution of Eq. (65) with energies lower than M_1+M_2. This is what is found, for instance, for the O(4) GN perturbed by the $\mathbb{Z}_2$ anisotropy, as discussed below.

E. Coupling of massive and massless modes

The situation close to the U(1) and $\mathbb{Z}_2$ critical points, described by Eq. (28) with $N_2=1,2$, is more tricky since some gapless modes are present. This problem was already addressed in Sec. V C and FFPT cannot add much to that analysis. Nevertheless, we find it instructive to briefly discuss the problem also in this framework. Let us look for simplicity at Eq. (28) with $N_1=3$, $N_2=1$ and uniform deformation $\delta g_{ab}=\delta g$. For $\delta g=0$ the spectrum consists of a massless Majorana mode and massive O(3) kinks. According to Eqs. (52) and (57) the mass variation is given by

$$\delta m_3 \simeq 2\delta g\langle\chi_R^a\chi_L^a\rangle F_{R,L}^{(\xi_R^3\xi_L^3)}(i\pi-\infty), \tag{82}$$

$$\delta m_\alpha^2 \simeq 2\delta g\langle\xi_R^3\xi_L^3\rangle_\alpha\langle\theta|\chi_R^a\chi_L^a|\theta\rangle_\alpha, \tag{83}$$

where the indices 3 and α indicate massless Majorana fermions and massive O(3) GN kinks, respectively. The VEV $\langle\chi_R^a\chi_L^a\rangle$ is different from zero and $F_{R,L}^{(\xi^3\xi^3)}(\theta)$ is constant for any value of θ; then from Eq. (82) it follows that the perturbation induces a mass linear in δg—i.e., as soon as the coupling is turned on a massive singlet appears in the spectrum.

One needs to be careful in the analysis of the second equation. In fact, $\langle\xi_R^3\xi_L^3\rangle$ vanishes in the unperturbed theory, implying that the mass variation of the kinks vanishes in the first order. Nevertheless, $\langle\xi_R^3\xi_L^3\rangle \sim \delta m_3$ and then Eq. (83) can still be applied, just keeping in mind that the effect on the kinks mass is of higher order in δg. Since the operator $(\chi_R^a\chi_L^a)$ is nonlocal with respect to the kinks, the RHS of Eq. (83) diverges and kinks confine. One should notice that besides the one considered in Eq. (83), there are other second-order contributions to the mass variation of the kinks; nevertheless, they will not be able to compensate the divergence and will not modify qualitatively the kink confinement. It can be shown that the confined states will always be unstable and then, in agreement with the semiclassical analysis, the only stable particles will be singlets and kinks with quantum numbers of the O($N+1$) model.

These results can also be checked using the opposite limit $\delta g \sim g_1=g_2$ and treating the model (28) as a perturbation of the O(4) GN (remember that for $N=4$ the GN model has only

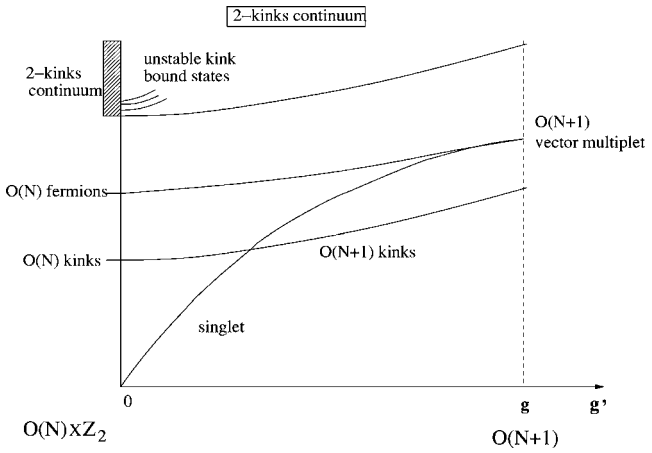

FIG. 3. A qualitative picture of the spectrum of the model interpolating between the $O(N)\times\mathbb{Z}_2$ and $O(N+1)$ GN models.

kinks in the spectrum). This perturbation is local with respect to the O(4) kinks and then produces an adiabatic change of their masses. At the same time we know that the O(4) model also contain (unstable) vector particles above the two-kink threshold. As described in the previous section we can use FFPT to check whether the perturbation induces further attraction that stabilizes them. Since the vector particles are bound states of kinks, for small deviations from the O(4) point we can write their wave function like Eq. (64), with a and b being O(4) kinks, and study the stability of the bound state by solving the eigenvalue equation (65). Even without entering into the details of the computation one can easily see that the form of the potential naturally split singlet and triplet bound states and in particular the interaction between kinks in the singlet state is attracting while the one between kinks in the triplet state repulsive. Then it turns out that the interaction stabilizes the singlet that will appear in the spectrum. This implies that the singlet state will be stable for any value of $\delta g < g_3$ and will cross the threshold at the O(4) point (see Fig. 3). We can repeat the same procedure for $N_1=5$; the main difference is that the unperturbed theory has fermionic states in the spectrum.

VIII. SPECTRUM AROUND THE PHASE BOUNDARIES

The analysis of the previous sections allows us to understand qualitatively, but rigorously, the spectrum of the model (2) close to the phase boundaries, where it can be seen as a perturbation of some integrable models.

A. From SCd to CDWd (SCs to CDW) phases through $\mathbb{Z}_2$ QCP

At the $\mathbb{Z}_2$ QCP the Hamiltonian (2) is described by a deformed O(5) GN model decoupled from the critical Ising model. The effect of the anisotropy is to lift the degeneracy between the vector particles. Away from the $\mathbb{Z}_2$ QCP the coupling is

$$-2(\xi_R^3\xi_L^3)\{g_{\sigma-}(\chi_R^a\chi_L^a)+g_{c,ss}[(\xi_R^1\xi_L^1)+(\xi_R^2\xi_L^2)]\}. \quad (84)$$

It is convenient to study the spectrum for $g_{\sigma,+}=g_{\rho,-}=g_{c,st}=g$ and $g_{\sigma-}=g_{c,ss}=g_X$ when the O(5) symmetry is exact. The RG equations

$$\dot{g}=-3g^2-g_X^2, \quad \dot{g}_X=-4g_Xg \quad (85)$$

have the following RG invariant: $C=(g^2-g_X^2)/g_X^{3/2}$. To understand the spectrum we can use results from the previous sections as well as the exact solution of the $(5+1)$ model presented in Appendix C. The spectrum consisted of $5+1$ vector particle multiplets and a quartet of kinks. The symmetry of the spectrum remains $O(5)\times\mathbb{Z}_2$ which corresponds to the splitting of the vector multiplet as $5+1$. Following the arguments of Sec. VII C we find that at large $C\gg 1$ the mass ratio of the different vector particles is $\sim g_X(m)\sim C^{-2/3}$. At $C\ll 1$ the vector multiplet approaches the O(6) symmetry with the splitting $\sim C$.

Then, in general, the SCd phase has kink particles with the O(6) quantum numbers and vector multiplet containing a triplet, doublet, and a singlet with different masses. All masses have the same sign. By going through $\mathbb{Z}_2$ QCP the singlet mass changes sign and one finds the orbital antiferromagnet (CDWd) phase.

B. From one SC (CDW) phase to another one through U(1) QCP

At the U(1) transition two Majorana fermions are massless and the rest is a deformed O(3) GN model equivalent, for small deformations, to the $3+1$ model discussed in Sec. VI. Thus the spectrum consists of the Gaussian massless mode, the SU(2) kink doublet, and a singlet particle of a lower mass. The $\Theta_c^{(-)}$ field acquires a mass gap as soon as the coupling between the two sectors is on. The effective field theory describing the lowest excitations is the sine-Gordon (SG) one:

$$S=\frac{1}{2}[\partial_\mu\Theta_c^{(-)}]^2+v\cos[\beta\Theta_c^{(-)}], \quad (86)$$

with $v=i\langle[g_{s,ct}(\chi_R^a\chi_L^a)+g_{c,ss}\xi_R^3\xi_L^3]\rangle$ and $\beta^2=4\pi(1-g_{\rho,-}/2\pi)^{-1}$. The SG kinks with period $2\pi/\beta$ constitute a low-lying doublet. Thus the vector multiplet is reduced to the U(1) doublet and the Majorana singlet. For $\beta^2>4\pi$ (repulsive interactions) there are no sine-Gordon bound states, but if $\beta^2<4\pi$, are also additional bound states (breathers). These particles are absent in the O(6) GN model. As far as the kinks are concerned, they acquire both spin and U(1) quantum numbers via creation of bound states between half (anti)kinks of $\Theta_c^{(-)}$ with period π/β and the SU(2) kinks.

C. Around the first-order line

At the first-order transition the spectrum consists of kinks with different masses M_1 and M_2 belonging to the isotropic and anisotropic $[U(1)\times\mathbb{Z}_2]$ O(3) GN models, respectively. As soon as the interaction is turned on all kinks confine and one has fermions close to the two kink thresholds $2M_1$ and $2M_2$ and new kinks close to the M_1+M_2 threshold. As we discussed earlier in Sec. VII A, the region of weak confinement, where one may observe several generations of kinks, is likely to be narrow.

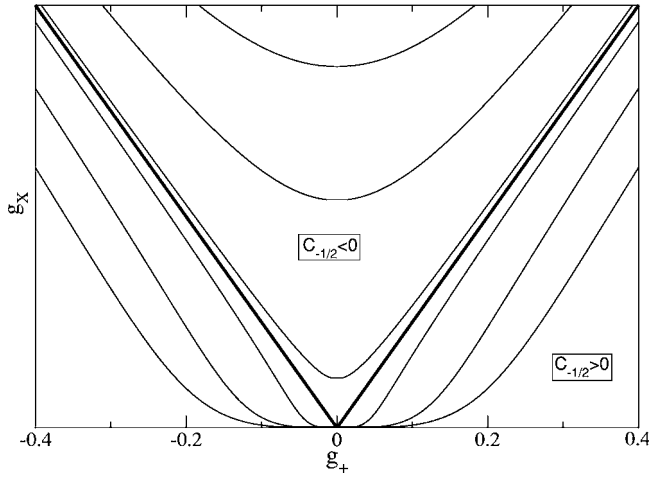

FIG. 4. RG flows (88) for $C_{1/2}=0$. The thick line represents the flow with $C_{-1/2}=0$.

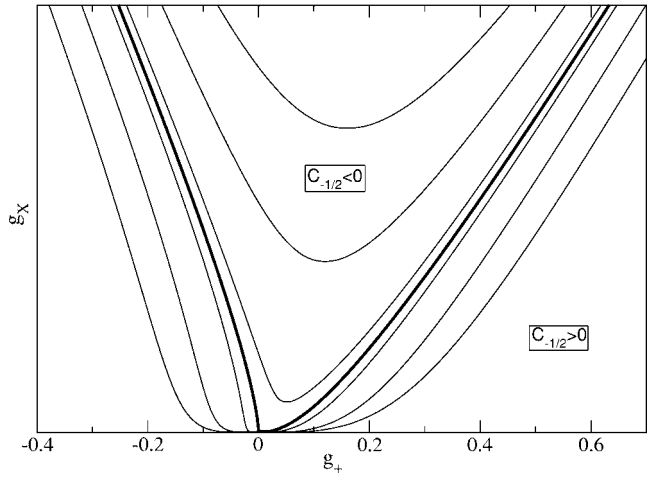

FIG. 5. RG flows (88) for $C_{1/2}>0$. The thick line represents the flow with $C_{-1/2}=0$.

IX. FURTHER FROM THE BOUNDARIES: O(3)×O(3) MODEL AS A SIMPLIFIED CASE

With the results of the previous sections at hand we will return to the case $N=6$ and consider the model (2) with a more symmetric form of the interaction

$$V=-g_+(\chi_R^a\chi_L^a)^2-2g_X(\chi_R^a\chi_L^a)(\xi_R^b\xi_L^b)-g_-(\xi_R^a\xi_L^a)^2, \quad (87)$$

as it was done in Refs. 10, 54, and 55. Though the subsequent RG analysis has a significant overlap with the one conducted in these papers, we include it here for completeness. The RG equations have the following form:

$$\dot{g}_+=g_+^2+3g_X^2, \quad \dot{g}_-=g_-^2+3g_X^2, \quad \dot{g}_X=2g_X(g_++g_-). \quad (88)$$

In this case we have managed to find the RG invariants explicitly:

$$C_{-1/2}=\frac{g_+g_--g_X^2}{\sqrt{|g_X|}}, \quad C_{1/2}=\frac{g_+-g_-}{2\sqrt{|g_X|}}. \quad (89)$$

For $g_a=g+\delta g_a$ these invariants correspond to the ones found in Sec. VII C. (see Figs. 4 and 5). If the O(3)×O(3) model is replaced by O(N)×O(N), the power 1/2 in Eqs. (89) is replaced by $(N-2)/(N-1)$ This means that in the large-N limit the ratios of coupling constants become RG invariants which coincides with conclusions of Sec. V. We also observe that a sign of the quadratic form γ is RG invariant which gives support to the $1/N$ analysis of Sec. V. Using these RG invariants one can integrate Eqs. (88). It should be kept in mind, however, that Eqs. (88) together with the explicit form (89) are valid only at $|g_a|<1$. As soon as one of the couplings becomes ~ 1 the scaling of this coupling should be stopped and the problem reconsidered.

The solution of this equation is given by

$$4t=\pm\int_{g_X(0)}^{g_X(t)}\frac{dg}{g\sqrt{C_{-1/2}g^{1/2}+C_{1/2}^2g+g^2}}, \quad (90)$$

which can be expressed in terms of elliptic functions of complex modulus and argument.

The phase diagram has three areas corresponding to different properties of the interaction tensor.

(i) The signature of the interaction tensor is positive: $C_{1/2}>0$ and $C_{-1/2}>0$. All couplings scale to zero.

(ii) The signature is negative ($C_{1/2}<0$) and $C_{-1/2}>0$. The system scales to strong coupling. The energy scale on which the spectral gaps are formed is given by

$$M\sim\Lambda\exp\left[-\pi\int_{|g_X(0)|}^{\infty}\frac{dg}{g\sqrt{C_{-1/2}g^{1/2}+C_{1/2}^2g+g^2}}\right]. \quad (91)$$

At $C_{-1/2}>0$ the integral in the exponent diverges at $g_X(0)\to 0$. Therefore the theory has a proper scaling limit $M=\text{const}\times g_X(0)\to 0$, $\Lambda\to\infty$. This limit is characterized by the RG invariants $C_{\pm 1/2}$. The case $C_{\pm 1/2}=0$ corresponds to the O(6) GN model. The opposite limit $\max(C_{\pm 1/2})\gg 1$ describes the O(3)×O(3) model in the regime of weak confinement (see Secs. V B and VII D).

(iii) $C_{-1/2}<0$. The system scales to strong coupling for any sign of the bare diagonal couplings. In this case the scaling trajectory for $g_X(t)$ bounces off its minimal value g^* given by the root of the equation

$$[g^*]^{3/2}+C_{1/2}^2[g^*]^{1/2}-|C_{-1/2}|=0. \quad (92)$$

If $g_X(0)>0$, the weakest interaction is achieved at the energy scale

$$E^*=\Lambda\exp\left[-\pi\int_{g^*}^{g_X(0)}\frac{dg}{g\sqrt{C_{-1/2}g^{1/2}+C_{1/2}^2g+g^2}}\right] \quad (93)$$

and the strong-coupling regime is reached at

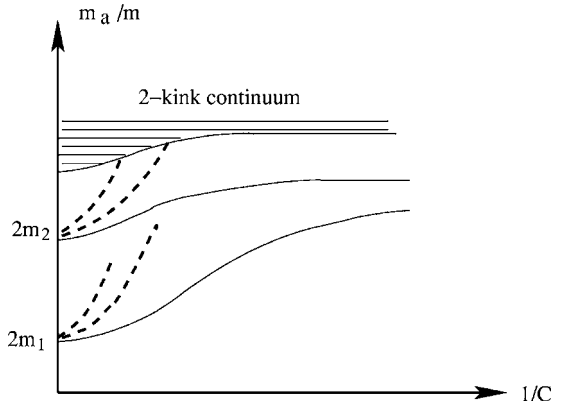

FIG. 6. The qualitative picture of the mass spectrum of the $O(3)\times O(3)$ GN model as a function $1/C_{1/2}$. The dashed lines show masses of mesons.

$$M = E^* \exp\left[-\pi \int_{g^*}^{\infty} \frac{dg}{g\sqrt{C_{-1/2}g^{1/2} + C_{1/2}^2 g + g^2}} \right]. \quad (94)$$

As we said in the Introduction, the maximal spectral gap corresponding to $g_X(0) \to +\infty$ is

$$M \sim E^{*2}/\Lambda. \quad (95)$$

Since the integral (90) never diverges at $C_{-1/2} < 0$, the RG time in which the strong-coupling limit is reached always remains finite. Therefore at finite $C_{-1/2} < 0$ the scaling limit does not exist.

If we relax conditions on the scaling limit, we can venture into the area $C_{-1/2} < 0$, as far as the spectral gaps remain much smaller than the bandwidth. For this we need g^* to be small which is achieved by making C_1 small. Thus the effective low-energy theory describing the state with emergent attraction is the $C_{-1/2}=0$ field theory with nonrelativistic corrections in M/Λ. The condition $C_{-1/2}=0$ does not put any restrictions on $C_{1/2}$; in the realistic two-leg ladder, where bare lattice interactions are not small, $C_{1/2}$ may have any value. Equation (89), pointing to small values of $C_{\pm 1/2}$ at small bare couplings, is not valid in that limit.

Taking the above into account we can qualitatively describe the overall spectrum of the $O(3)\times O(3)$ using results of Secs. VII C and VII D. The results are summarized in Fig. 6.

A. Mass is induced in the otherwise massless sector

It remains to study the situation when some coupling constants are much larger than the others such that they reach the strong-coupling limit first. This analysis is complementary to the one of Secs. V C and VII E. In this case one should study the spectrum using two-stage RG. There are two cases to consider.

(i) One of the sectors is massless at $g_X=0$. Let it be the $+$ sector $g_-(0) < 0, g_+ > 0$, so that at $g_X=0$ the interaction in χ_a sector is marginally irrelevant. The condition $C_{-1/2} < 0$ is fulfilled. As we shall demonstrate, the vector particles do appear in this sector at $g_X \neq 0$, but the symmetry is not restored.

(ii) Both sectors are massive at $g_X=0$. Let $0 < |g_X(0)| \ll g_+(0)g_-(0)$ and $-g_+(0) \sim -g_-(0) > 0$. Then the coupling $g_X(M)$ is still weak. Following the arguments of the previous sections, we conclude that the interaction leads to the creation of generations of O(6) kinks with masses close to $M_1 + M_2$ and the formation of two generations of the vector particles: one with masses close to $2M_1$ and the other one with masses close to $2M_2$.

We use the two-stage RG. Let M_3 is the mass scale of the O(3) GN model in the $-$ sector. At this energy the renormalization of g_- coupling terminates and a nonzero average is formed:

$$i\langle \xi_R^b(M_3^{-1})\xi_L^b(0)\rangle \approx -M_3. \quad (96)$$

Replacing the $\bar{\xi}\xi$ operator by its average in the low-energy effective action for χ fermions we obtain the effective action like Eq. (44) with the UV cutoff M_3:

$$\mathcal{L}_{eff} = \frac{i}{2}\bar{\chi}_a \gamma_\mu \partial_\mu \chi_a + iM_0 \bar{\chi}_a \chi_a - g_+(M_3)(\bar{\chi}_a \chi_a)^2, \quad (97)$$

where $M_0 = ig_X(M_3)\langle \xi_R^b(M_3^{-1})\xi_L^b(0)\rangle$. The form of this Hamiltonian suggests that the vector triplet in the $-$ sector is stabilized. For the procedure to be self-consistent the mass of this vector particle should be $M_+ \ll M_3$. Let us assume that $g_+(M_3)$ is still positive, which is the case at sufficiently small $g_X(0)$. Then the downward renormalization of g_+ will continue until the energy M_+ (the resulting mass for χ fermions). The latter is determined by the equation

$$M_+ = \frac{M_0}{1 + \dfrac{g_+(M_3^{-1})}{4\pi}\ln(M_3/M_+)}. \quad (98)$$

We see that the presence of the repulsion in the $+$ channel can further reduce the mass of the vector particle. The model (97) was introduced in Ref. 56 to describe low-energy properties of the spin $S=1$ Heisenberg antiferromagnetic chain.

B. 4+2 splitting

The trickiest and at the same time the most realistic case is when the modes split as $2+4$ with repulsive interaction between the four magnetic modes. In this case neither group can produce a mass gap and the gap is generated solely by the interaction. This happens, for instance, in the model with no interchain tunneling in the presence of the density-density interaction. Then only the $2k_F$ components of the density interact, leading to the arrangement

$$g_{\sigma,+} = g_{\sigma,-} \equiv v > 0, \quad g_{c,ss} = g_{c,st} \equiv g,$$

where v originates from the intrachain exchange interaction. The O(6) symmetry is split as $O(4)\times U(1)$

$$ig\cos\beta\Theta_c^{(-)} \sum_{a=0}^{3} \chi_R^a \chi_L^a + v(i\chi_R^a \chi_L^a)^2. \quad (99)$$

The RG equations

$$\dot{g}_{\rho,-} = -4g^2, \quad \dot{v} = -2v^2 - 2g^2, \quad \dot{g} = -g(g_{\rho,-} + 3v), \tag{100}$$

where $\beta^2/4\pi = 1 + g_{\rho,-}/2\pi$. In the realistic case of repulsion $g_{\rho,-} < 0$ the system scales to strong coupling with v changing sign. Assuming that $-g_{\rho,-}$ is the largest among the coupling constants and neglecting its renormalization we arrive at the approximate solution

$$g = g(0)e^{|g_{\rho,-}|t}, \quad v = v(0) - \frac{g^2(0)}{|g_{\rho,-}|}(e^{2|g_{\rho,-}|t} - 1), \tag{101}$$

such that v changes sign at

$$t^* \approx \frac{1}{2|g_{\rho,-}|} \ln\left[\frac{|g_{\rho,-}|v(0)}{g^2(0)} + 1\right], \tag{102}$$

which fixes the upper limit for the gaps $E^{*2}/\Lambda \sim \Lambda e^{-2t^*}$. This corresponds to the scenario when the mass is generated by the effective attraction among the fermions.

At small $d = \beta^2/4\pi < 1/2$ another scenario can be realized. To understand the spectrum we resort to a $1/N$ approximation where N is the number of fermion species. Assuming that the fermion masses are larger than the boson ones, we integrate over fermions and obtain the following effective potential for $\Theta_c^{(-)} \equiv \phi$ field:

$$V = -\frac{g^2 N}{4\pi} \cos^2(\beta\phi) \ln\left[\frac{\Lambda}{g|\cos(\beta\phi)|}\right], \tag{103}$$

which can be approximated as a pure cosine. This potential is relevant only when $d < 1/2$ and for $d > 1/4$ the spectrum contains only kinks. Let us call their mass gap m_ϕ. Then the estimate for the fermion gap is

$$m_\chi \approx g\langle\cos(\beta\phi)\rangle = gC_\beta\Lambda(m_\phi/\Lambda)^d, \tag{104}$$

where C_β is a constant. The fermion gap is indeed much larger than the kinks gap which justifies the integration over the fermionic modes. Thus the spectrum in this case consists only of the O(6) kinks. The kinks acquire quantum numbers from the spinor representation of the O(6) group through attachment of the fermions zero modes (see Sec. V).

X. CORRELATION FUNCTIONS AND EXPERIMENTAL PROBES

A detailed analysis of correlation functions is outside the scope of this paper, so we restrict this discussion to some qualitative remarks.

Among the available experimental methods the ones which probe correlations functions at various frequencies and momenta are angle-resolved photoemission spectroscopy (ARPES) and inelastic neutron and x-ray scattering. All other probes measure either local correlation functions [nuclear magnetic resonance (NMR), tunneling spectroscopy] or correlation functions at zero momenta (optical conductivity, Raman scattering).

The only known system which the effective Hamiltonian resembles the one for a single two-leg ladder are single wall carbon nanotubes. However, though the doped nanotube is described by the effective Hamiltonian (2),[57] the values of the bare couplings for the nanotubes of available size are such that the gaps are extremely small. In other experimentally available systems, such as the telephone number compound mentioned in Introduction, ladders are packed into a three-dimensional (3D) arrangement. In that case interactions of gapless charge modes from different ladders may lead to 3D ordering.

Let us discuss the behavior of correlation functions above 3D phase transition (if such transition occurs). In this case both $\Phi_c^{(+)}$ and $\Theta_c^{(+)}$ exponents have power-law correlation functions. Since these exponents enter the majority of experimentally measurable correlation functions, emission of all massive excitations is accompanied by emission of gapless bosonic modes. This makes the massive particles incoherent. The best one can do at the circumstances is to look for operators whose correlation functions contain matrix elements corresponding to emission of just one massive particle (and, of course, a cascade of gapless bosons).

Having this in mind, let us consider, for example, the SCd phase. In this phase all σ (μ) fields are locked together with $\cos[\sqrt{\pi}\Theta_c^{(-)}]$(sin). Then the operators with matrix elements between the vacuum and a single-particle state of the doublet-vector particle are the Fourier components of the particle density at $2k_F^{(p)}$:

$$\rho(2k_F^{(p)}) = \sum_\sigma R^+_{\sigma,p} L_{\sigma,p} \sim i e^{i\sqrt{\pi}\Phi_c^{(+)}} e^{\pm i\sqrt{\pi}\Phi_c^{(-)}} [\sigma_1\sigma_2\sigma_3\sigma_0 \mp \mu_1\mu_2\mu_3\mu_0]. \tag{105}$$

As far as the magnetic triplet is concerned, it is emitted at $2(k_F^{(1)} + k_F^{(2)})$ by the magnetization operator

$$S^a(2k_F) = R^+_{0,\sigma}\sigma^a_{\sigma\sigma'}L_{\pi,\sigma'} = \frac{1}{2\pi a} e^{i\sqrt{\pi}\Phi_c^{(+)}} e^{i\sqrt{\pi}\Theta_c^{(-)}} [N_a\mu_0 + M_a\sigma_0], \tag{106}$$

where

$$N^a = (\mu_1\mu_2\sigma_3, \mu_1\sigma_2\mu_3, \sigma_1\mu_2\mu_3),$$

$$M^a = (\sigma_1\sigma_2\mu_3, \sigma_1\mu_2\sigma_3, \mu_1\sigma_2\sigma_3).$$

The corresponding quasicoherent peaks disappear below T_c since the $\Theta_c^{(+)}$ is locked and correlations of $e^{i\sqrt{\pi}\Phi_c^{(+)}}$ become short ranged. However, if the SCd phase is replaced at stronger interactions by the $4k_F$-ordered Wigner crystal (recall the discussion in Sec. II B), it is $\Phi_c^{(+)}$ field which is locked. Then the all the above peaks become sharp (this was in fact observed in the telephone number compound[58]).

XI. CONCLUSIONS

In this paper we made an attempt to outline the picture of the excitation spectrum of a field theory with a symmetry of a doped two-leg ladder: namely, the anisotropic O(6) Gross-Neveu model. This model is not integrable, and then it is not possible to obtain exact results except for some specific

points in parameter space. We combined information coming from the RG analysis with semiclassical methods and form-factor perturbation theory. It follows from our analysis that throughout most of the phase diagram the spectrum consists of degenerate quartets of kinks and antikinks and the multiplet of vector particles split as $3+2+1$. This basic picture experiences corrections when one moves through the phase diagram. Namely, in some areas of the phase diagram the splitting is extremely small, while in some others it may become so large that some multiplets are pushed in the continuum and become unstable. The phase diagram presents different types of quantum critical points. At second-order transition lines masses of certain particles vanish. Very close to the first-order transition line additional generations of kinks emerge. Strong interactions in some sectors may generate additional bound states (like breathers in the asymmetric charge sector).

As we have mentioned many times throughout the text, one potential application of this theory is "telephone number" compound $Sr_{14-x}Ca_xCu_{24}O_{41}$. This is undoubtedly a strongly correlated system. The measurements of low-frequency dielectric and optical response demonstrate existence of a weakly pinned phason mode,[6,8] which we identified as the $\Phi_c^{(+)}$ mode. At the same time such probes as NMR,[3] inelastic neutron scattering (Ref. 4) and ARPES (Ref. 5) show gaps in all other parts of the spectrum. This is in agreement with existing theoretical understanding of the ladder materials.

The question of the validity of the quasi-one-dimensional field theory description is decided by (i) comparison between the values of the gaps and the bandwidth and by (ii) presence of essentially one-dimensional effects, such as different gap values for different channels. The field theory is valid when the gaps are small compared to the bandwidth. The gaps extracted from the ARPES measurements were obtained only for $x=0$ where the number of holes is apparently rather small (though not zero, since according to Ref. 8 the gapless CDW mode exists at this concentration). The ARPES shows the single-electron gap ~ 0.3 eV and the bandwidth ~ 1.2 eV.[5] At the same time the neutron scattering (also available only for $x=0$) gives the spin-triplet gap ~ 32 meV with the bandwidth for the spin excitations ~ 200 meV. NMR measurements done in a broad range of Ca concentrations show that the spin gap decreases with doping and becomes less than 200 K at $x>3$. The absence of temperature saturation of the magnetic susceptibility indicates a crossover to the paramagnetic regime, meaning that gaps for nonmagnetic excitations also become smaller at these x. Therefore the gap/bandwidth ratios are sufficiently small for the field theory description to be valid.

On the other hand, the optical conductivity measurements indicate the presence of essentially one-dimensional effects. They show a strong peak at radio frequencies (presumably coming from the phason mode) and a threshold at infrared frequencies (the so-called CDW gap). If the CDW state would form as a result of Fermi surface instability, as happens in three-dimensional systems with nested Fermi surfaces, this gap would be twice as large as the single-particle gap measured by ARPES. It would also coincide with the spin gap. However, according to Ref. 59, the values of the CDW gaps at $x=0$, 3, and 9 are 130 meV, 110 meV, and 3 meV, respectively, which is either several times larger or much smaller than the spin gap. From this analysis we conclude that though detailed comparison between theory and experiment would be premature, the field theory description of the telephone number compound is a reasonable approach (as far as the system remains strongly one dimensional which probably corresponds to $x<9$).

We believe that the present experiments allow one to determine the part of the phase diagram where the telephone number compound is located. The recent x-ray measurements show that the holes may crystallize in a three-dimensional Wigner crystal[9,60] (the use of the term is explained in Ref. 32). Since the particle peaks sharpen below the transition, we take it as an indication that this is a $4k_F$ Wigner crystal replacing the SCd phase, as described in Sec. III. Such a crystal exists only if the electron-electron interaction has a long-range tail. This points towards the standard Coulomb interaction as the primary agent of its formation. Such an interaction may lead to relatively small values of β^2 and consequently to new bound states. It is just possible that one such bound state (a breather in the $\Theta_c^{(-)}$ sector) appears as a sharp peak in the Raman scattering experiments.[61]

ACKNOWLEDGMENTS

We are grateful to P. Azaria, M. J. Bhaseen, G. Blumberg, F. Essler, M. Fabrizio, E. Gava, T. Grava, R. M. Konik, P. Lecheminant, S. Lukyanov, G. Mussardo, A. A. Nersesyan, T. M. Rice, G. Sotkov, F. A. Smirnov, and A. B. Zamolodchikov with whom various aspects of this work were discussed on different stages and for help with and interest in the work. A.M.T. acknowledges the support from the U.S. DOE under Contract No. DE-AC02-98 CH 10886 and is grateful to Abdus Salam ICTP and Princeton University for their hospitality. D.C. acknowledges hospitality and support from the Institute for Strongly Correlated and Complex Systems at BNL.

APPENDIX A: BOSONIZATION

We adopt the following notations:

$$R_{p,\sigma}=\frac{\eta_{p\sigma}}{\sqrt{2\pi a_0}}e^{-i\sqrt{4\pi}\varphi_{p\sigma}},\quad L_{p,\sigma}=\frac{\eta_{p\sigma}}{\sqrt{2\pi a_0}}e^{i\sqrt{4\pi}\bar{\varphi}_{p\sigma}}, \quad \text{(A1)}$$

where $p=\pm 1$ and φ and $\bar{\varphi}$ are bosonic fields with right and left chirality. The Klein factors satisfy anticommutation relations of the O(4) Clifford algebra

$$\{\eta_a,\eta_b\}=\delta_{ab}$$

and can be chosen as follows:[20]

$$\eta_{-1\sigma}\eta_{1\sigma}=i,\quad \eta_{p\uparrow}\eta_{p\downarrow}=i(-1)^{(p+1)/2}. \quad \text{(A2)}$$

The chiral bosonic fields are decomposed into the normal modes as follows:

$$\varphi_{p\sigma}=\frac{1}{2}\{[\phi_c^{(+)}+p\phi_c^{(-)}]+\sigma[\phi_s^{(+)}+p\phi_s^{(-)}]\}, \quad \text{(A3)}$$

with the same decomposition for $\bar{\varphi}$. The bosonic field Φ and its dual Θ as usual are

$$\Phi_{s,c}^{(\pm)} = \phi_{s,c}^{(\pm)} + \bar{\phi}_{s,c}^{(\pm)}, \quad \Theta_a^{(\pm)} = \phi_{s,c}^{(\pm)} - \bar{\phi}_{s,c}^{(\pm)}. \tag{A4}$$

The Ising model order and disorder parameter fields σ and μ are related to the bosonic fields as follows:

$$\cos[\sqrt{\pi}\Phi_s^{(+)}] = \sigma_1\sigma_2, \quad \sin[\sqrt{\pi}\Phi_s^{(+)}] = \mu_1\mu_2,$$

$$\cos[\sqrt{\pi}\Theta_s^{(+)}] = \mu_1\sigma_2, \quad \sin[\sqrt{\pi}\Theta_s^{(+)}] = \sigma_1\mu_2, \tag{A5}$$

with the similar formulas relating $\Phi_s^{(-)}$, $\Theta_s^{(-)}$ to $\sigma_3, \sigma_0, \mu_3, \mu_0$.

APPENDIX B: SEMICLASSICAL ANALYSIS OF GENERALIZED O($2n$) GN MODELS

In order to have a more intuitive picture of the effect of perturbations (26) and (28) on GN models we repeat the semiclassical analysis of Sec. V for N and M even, $N=2n$ and $M=2m$, following Ref. 34. The advantage of this assumption lies in the fact the Majorana fermions can be bosonized in couples and then the potential of the O($2n$) GN model (4) takes the form

$$V = -g'\left(\sum_{i=1}^{n} \cos(\sqrt{4\pi}\phi_i)\right)^2. \tag{B1}$$

It has two families of minima, $\phi_i = \sqrt{\pi}n$ and $\phi_i = \sqrt{\pi}(n+1/2)$, which are usually referred to as positive and negative vacua because they correspond to positive and negative values of $\Sigma_a \psi_R^a \psi_L^a = \Sigma_i \cos\sqrt{4\pi}\phi_i$. Fermionic excitations (when stable) correspond to configurations interpolating between minima that belong to the same family—for instance, from a configuration (0,…,0) at $x \to -\infty$ to $(\pm\sqrt{\pi}, 0, \ldots, 0)$ at $x \to +\infty$. On the other hand, kinks interpolate between minima of different families—for example, from (0,…,0) for $x \to -\infty$ to $(\pm\sqrt{\pi}/2, \ldots, \pm\sqrt{\pi}/2)$ for $x \to +\infty$. It is easy to see that, while there are N possible fermionic states, the number of kinks states is 2^n. Note that since kinks interpolate between positive and negative vacua, the mean value of $\psi_R^a \psi_L^a$ changes sign along a kink configuration.

From this picture it is clear that fermions can be considered as bound states of kinks. In fact, for instance, an elementary excitation associated with the transition $(0, \ldots, 0) \to (\sqrt{\pi}, 0, \ldots, 0)$ can be obtained also with two transitions $(0, \ldots, 0) \to (+\sqrt{\pi}/2, \ldots, +\sqrt{\pi}/2) \to (\sqrt{\pi}, 0, \ldots, 0)$, where each of the two jumps corresponds to a kink. The stability of fermions against the decay into a pair of kinks depends on N.

Let us now first consider the effect of a simple perturbation of the form

$$V' = -\sum_i \cos\sqrt{4\pi}\phi_i. \tag{B2}$$

Here the positive and negative minima are split and only the former remain absolute minima. This implies that kinks interpolating between different families are not present anymore and the model has only fermionic excitations. This is a simple example of confinement. If we now consider the model (28), the effect of the perturbation on the excitations of the two GN models, originally decoupled, is somewhat similar. When the two models are decoupled each of them has the same families of minima described above. For instance, if we introduce ϕ_i and σ_i associated with the χ^a's and ξ^b's, respectively, configurations like $(\phi_1, \ldots, \phi_n; \sigma_1, \ldots, \sigma_n) = (0, \ldots, 0; \pm\sqrt{\pi}/2, \ldots, \pm\sqrt{\pi}/2)$ are absolute minima. Nevertheless, this does not remain true in presence of a perturbation of the form

$$\delta\tilde{g}_{a,b} \cos\sqrt{4\pi}\phi_a \cos\sqrt{4\pi}\sigma_b \tag{B3}$$

(here we assume that also the perturbation is such that it can be written in a simple bosonic form). Again the kinks of the two decoupled GN models confine and disappear from the spectrum. At the same time, together with fermions, new kinks with the quantum number of O($N+M$) GN appear. They interpolate between configurations like $(0, \ldots, 0; 0, \ldots, 0) \to (\pm\sqrt{\pi}/2, \ldots, \pm\sqrt{\pi}/2; \pm\sqrt{\pi}/2, \ldots, \pm\sqrt{\pi}/2)$, which remain degenerate minima also of the perturbed theory. Fermionic excitations of the two models remain stable.

Following the same arguments one can easily see that in presence of perturbations of the form (26) the O(N) kinks remain stable. In fact, the potential

$$\delta g_{a,b} \cos\sqrt{4\pi}\phi_a \cos\sqrt{4\pi}\phi_b \tag{B4}$$

does not lift the degeneracy of the minima of the unperturbed GN model.

APPENDIX C: THE EXACT SOLUTION OF 5+1 AND 3+1 MODELS

In this appendix we describe the S-matrix of two models, which we call the 5+1 and 3+1 models, with $O(5) \times \mathbb{Z}_2$ and $O(3) \times \mathbb{Z}_2$ symmetry, respectively. The latter was introduced and studied in detail in Refs. 42 and 43. The central charge in the UV computed with the thermodynamic Bethe ansatz is $c_{5+1}=3$ and $c_{3+1}=2$. The relationship with the models of interest in the paper is discussed in Sec. VI.

The spectrum of the 5+1 model consists of a singlet Majorana fermion with mass m_0, a quintet of Majorana fermions with masses $\sqrt{3}M$, and a quartet of kinks $\equiv$ antikinks (spinor particles) with mass M. The S-matrix for the 5+1 model is

$$S_{5+1} = \begin{pmatrix} S_{vv} & S_{vs} & -I \\ S_{vs} & S_{ss} & \xi\delta_\alpha^{\bar{\alpha}} \\ -I & \xi\delta_\alpha^{\bar{\alpha}} & -1 \end{pmatrix}, \tag{C1}$$

where

$$\xi(\theta) = \frac{e^{3\theta} - i}{e^{3\theta} + i}$$

and S^{vv}, S^{vs}, and S^{ss} are the O(5) S-matrices of vector and spinor particles. The above S-matrices were found in Refs. 38 (for the vector particles) and 39 (for kinks). The spinor S-matrix has the following form:

$$S^{ss}(\theta) = f(\theta)\left[\hat{P}_{asym} + \frac{\theta + i\pi/3}{\theta - i\pi/3}\hat{P}_v + \frac{\theta + i\pi}{\theta - i\pi}\hat{P}_0\right], \tag{C2}$$

where P_0, P_v, and P_{asym} represent projectors onto singlet, vector, and antisymmetric tensor representations and

$$f(\theta)=\frac{\Gamma\left(1+\frac{i\theta}{2\pi}\right)\Gamma\left(\frac{1}{2}-\frac{i\theta}{2\pi}\right)\Gamma\left(\frac{5}{6}-\frac{i\theta}{2\pi}\right)\Gamma\left(\frac{1}{3}+\frac{i\theta}{2\pi}\right)}{\Gamma\left(1-\frac{i\theta}{2\pi}\right)\Gamma\left(\frac{1}{2}+\frac{i\theta}{2\pi}\right)\Gamma\left(\frac{5}{6}+\frac{i\theta}{2\pi}\right)\Gamma\left(\frac{1}{3}-\frac{i\theta}{2\pi}\right)}.$$

The S-matrix has one physical pole on the physical strip ($0<\mathrm{Im}\,\theta<\pi$) at $\theta=i\pi/3$ corresponding to the vector particle and one unphysical at $2\pi i/3$. Each of the S-matrices is crossing symmetric, including the scalar factor ξ: $\xi(\theta)=-\xi(i\pi-\theta)$.

For the (3+1) model we have a similar structure:

$$S_{3+1}=\begin{pmatrix}[S^{SU(2)}]^{\bar{\alpha},\bar{\beta}}_{\alpha,\beta} & \xi\delta^{\bar{\alpha}}_{\alpha}\\ \xi\delta^{\bar{\alpha}}_{\alpha} & -1\end{pmatrix}, \tag{C3}$$

where

$$\xi(\theta)=\frac{e^{\theta}-i}{e^{\theta}+i}$$

and $S^{SU(2)}$ is the S-matrix of SU(2) Thirring model solitons.

APPENDIX D: SOLUTION OF THE LINEARIZED RG EQUATIONS

The RG equations (5) can be simplified for $g_a=g+\delta g_a$ with $g/\delta g_a\ll 1$. Defining for simplicity of notations $\delta g_a\equiv x_a$ we find that, to first order in $\mathbf{x}$ Eqs. (5) take the form

$$\frac{\dot{\mathbf{x}}}{2g}=-D\mathbf{x}, \tag{D1}$$

where

$$D=\begin{pmatrix}0 & 1 & 0 & 3 & 0\\ 1/2 & 1/2 & 3/2 & 3/2 & 0\\ 0 & 1 & 1 & 1 & 1\\ 1/2 & 1/2 & 1/2 & 3/2 & 1\\ 0 & 0 & 1 & 2 & 1\end{pmatrix} \tag{D2}$$

and g is solution of $\dot{g}=-4g^2$ and has the form

$$g(t)=\frac{1}{4t-g_0^{-1}}. \tag{D3}$$

It is convenient to introduce $\mathbf{y}$

$$\mathbf{x}=T\mathbf{y}, \tag{D4}$$

which satisfies the equation

$$\dot{\mathbf{y}}=-T^{-1}DT\mathbf{y}2g(t),\quad \mathbf{y}(0)=T^{-1}\mathbf{x}(0)\equiv A_a, \tag{D5}$$

where

$$T=\begin{pmatrix}-3 & -6 & -1 & 2 & 1\\ 3 & 3 & -1 & -1 & 1\\ -2 & -2 & 0 & -2 & 1\\ 0 & 1 & 0 & 1 & 1\\ 1 & 0 & 1 & 0 & 1\end{pmatrix} \tag{D6}$$

is chosen such that $T^{-1}DT=\mathrm{diag}(\lambda_1,\lambda_2,\lambda_3,\lambda_4,\lambda_5)$, with λ's being the eigenvalues of Eq. (D2), $\lambda_1=\lambda_2=-1$, $\lambda_3=\lambda_4=1$, and $\lambda_5=4$. Since the eigenvectors of degenerate eigenvalues are linearly independent, all solutions of Eq. (D5) have the form

$$y_a=A_a\exp[-\lambda_a l(t)], \tag{D7}$$

where

$$l(t)=\frac{1}{2}\ln(g_0^{-1})-\frac{1}{2}\ln(g_0^{-1}-4t). \tag{D8}$$

From this it follows that

$$y_a=A_a\left(\frac{1}{g_0}\right)^{\lambda_a/2}[\ln(\varepsilon/m)+1]^{-\lambda_a/2}, \tag{D9}$$

where the relationship between t and ε was used. The solution of Eq. (D1) can be obtained inverting Eq. (D4).

[1] E. Dagotto and T. M. Rice, Science **271**, 618 (1996).

[2] M. Uehara, T. Nagata, J. Akimitsu, H. Takahashi, N. Mori, and K. Kinoshita, J. Phys. Soc. Jpn. **65**, 2764 (1996); T. Nagata, M. Uehara, J. Goto, N. Komiya, J. Akimitsu, N. Motoyama, H. Eisaki, S. Uchida, H. Takahashi, T. Nakanishi, and N. Mori, Physica C **282-287**, 153 (1997).

[3] T. Imai, K. R. Thurber, K. M. Shen, A. W. Hunt, and F. C. Chou, Phys. Rev. Lett. **81**, 220 (1998).

[4] R. S. Eccleston, M. Uehara, J. Akimitsu, H. Eisaki, N. Motoyama, and S. I. Uchida, Phys. Rev. Lett. **81**, 1702 (1998).

[5] T. Takahashi, T. Yokoya, A. Ashihara, O. Akaki, H. Fujisawa, A. Chainani, M. Uehara, T. Nagata, J. Akimitsu, and H. Tsunetsugu, Phys. Rev. B **56**, 7870 (1997).

[6] B. Gorshunov, P. Haas, T. Rõõm, M. Dressel, T. Vuletić, B. Korin-Hamzić, S. Tomić, J. Akimitsu, and T. Nagata, Phys. Rev. B **66**, 060508(R) (2002).

[7] G. Blumberg, P. Littlewood, A. Gozar, B. S. Dennis, N. Motoyama, H. Eisaki, and S. Uchida, Science **297**, 584 (2002).

[8] A. Gozar, G. Blumberg, P. B. Littlewood, B. S. Dennis, N. Motoyama, H. Eisaki, and S. Uchida, Phys. Rev. Lett. **91**, 087401 (2003).

[9] P. Abbamonte, G. Blumberg, A. Rusydi, A. Gozar, P. G. Evans, T. S. Siegrist, L. Venema, H. Eisaki, E. D. Isaacs, and G. A. Sawatzky, Nature (London) **431**, 1078 (2004).

[10] P. Azaria, A. O. Gogolin, P. Lecheminant, and A. A. Nersesyan, Phys. Rev. Lett. **83**, 624 (1999).

[11] L. Balents and M. P. A. Fisher, Phys. Rev. B **53**, 12133 (1996).

[12] H. H. Lin, L. Balents, and M. P. A. Fisher, Phys. Rev. B **58**, 1794 (1998).
[13] C. Wu, W. V. Liu, and E. Fradkin, Phys. Rev. B **68**, 115104 (2003).
[14] M. Tsuchiizu and Y. Suzumura, J. Phys. Soc. Jpn. **73**, 804 (2004); cond-mat/0406430 (unpublished).
[15] D. Shelton and A. M. Tsvelik, Phys. Rev. B **53**, 14036 (1996).
[16] H. C. Lee, P. Azaria, and E. Boulat, Phys. Rev. B **69**, 155109 (2004).
[17] A. A. Nersesyan and G. E. Vachnadze, J. Low Temp. Phys. **77**, 293 (1989).
[18] I. Affleck and J. B. Marston, Phys. Rev. B **37**, R3774 (1998); J. B. Marston and I. Affleck, *ibid.* **39**, 11538 (1989).
[19] T. Giamarchi, *Quantum Physics in One Dimension* (Clarendon, Oxford, 2004).
[20] J. O. Fjaerestad, J. B. Marston, and U. Schollwöck, cond-mat/0412709 (unpublished).
[21] D. V. Khveshchenko and T. M. Rice, Phys. Rev. B **50**, 252 (1994).
[22] M. Troyer, H. Tsunetsugu, and T. M. Rice, Phys. Rev. B **53**, 251 (1996).
[23] D. Poilblanc, E. Orignac, S. R. White, and S. Capponi, Phys. Rev. B **69**, 220406(R) (2004).
[24] E. Orignac and T. Giamarchi, Phys. Rev. B **56**, 7167 (1997).
[25] R. Assaraf, P. Azaria, E. Boulat, M. Caffarel, and P. Lecheminant, Phys. Rev. Lett. **93**, 016407 (2004).
[26] R. M. Konik, H. Saleur, and A. W. W. Ludwig, Phys. Rev. B **66**, 075105 (2002).
[27] See, for instance, S. Coleman, *Aspects of Symmetry* (Cambridge University Press, Cambridge, England, 1985).
[28] G. Delfino, G. Mussardo, and P. Simonetti, Nucl. Phys. B **473**, 469 (1996).
[29] D. G. Shelton, A. A. Nersesyan, and A. M. Tsvelik, Phys. Rev. B **53**, 8521 (1996).
[30] A. O. Gogolin, A. A. Nersesyan, and A. M. Tsvelik, *Bosonization in Strongly Correlated Systems* (Cambridge University Press, Cambridge, England, 1999); A. M. Tsvelik, *Quantum Field Theory in Condensed Matter Physics* (Cambridge University Press, Cambridge, England, 2003).
[31] D. Gross and A. Neveu, Phys. Rev. D **10**, 3235 (1974).
[32] The term Wigner crystal is used to denote an ordered state where the spatial order originates from the electron-electron interactions. In quasi-one-dimensional systems such ordering does not necessarily require that the average Coulomb energy be much greater than the kinetic one. Therefore the density oscillations in quasi-1D Wigner crystals may be almost sinusoidal, unlike in an isotropic case.
[33] S. R. White, I. Affleck, and D. J. Scalapino, Phys. Rev. B **65**, 165122 (2002).
[34] R. Shankar and E. Witten, Nucl. Phys. B **141**, 349 (1978).
[35] R. F. Dashen, B. Hasslacher, and A. Neveu, Phys. Rev. D **12**, 2443 (1975).
[36] R. Jakiw and C. Rebbi, Phys. Rev. D **13**, 3398 (1976).
[37] E. Witten, Nucl. Phys. B **142**, 285 (1978).
[38] A. B. Zamolodchikov and Al. B. Zamolodchikov, Ann. Phys. (N.Y.) **120**, 253 (1979).
[39] E. Ogievetsky, N. Reshetikhin, and P. Wiegmann, Nucl. Phys. B **280**, 45 (1987).
[40] M. Karowsky and H. J. Thun, Nucl. Phys. B **190**, 61 (1981).
[41] P. Fendley and H. Saleur, Phys. Rev. D **65**, 025001 (2002).
[42] A. M. Tsvelik, Sov. Phys. JETP **66**, 754 (1987).
[43] N. Andrei and A. Jerez, Phys. Rev. Lett. **74**, 4507 (1995); N. Andrei, M. R. Douglas, and A. Jerez, Phys. Rev. B **58**, 7619 (1998).
[44] F. A. Smirnov and A. M. Tsvelik, Phys. Rev. B **68**, 144412 (2003).
[45] A. M. Tsvelik, Sov. J. Nucl. Phys. **47**, 172 (1988).
[46] Y. Y. Goldschmidt, Phys. Rev. Lett. **56**, 1627 (1986).
[47] F. A. Smirnov, *Form Factors in Completely Integrable Models of Quantum Field Theory* (World Scientific, Singapore, 1992); M. Karowski and P. Weisz, Nucl. Phys. B **139**, 455 (1978); B. Berg, M. Karowski, and P. Weisz, Phys. Rev. D **19**, 2477 (1979); V. P. Yurov and A. B. Zamolodchikov, Int. J. Mod. Phys. A **6**, 3429 (1991).
[48] Al. B. Zamolodchikov, Nucl. Phys. B **358**, 524 (1991).
[49] G. Delfino, G. Mussardo, and P. Simonetti, Phys. Rev. D **51**, R6620 (1995).
[50] D. Controzzi and G. Mussardo, Phys. Lett. B **617**, 133 (2005).
[51] R. Konik (private communication).
[52] P. Fonseca and A. B. Zamolodchikov, J. Stat. Phys. **110**, 527 (2003).
[53] L. D. Landau and E. M. Lifshitz, *Quantum Mechanics* (Pergamon, New York, 1991).
[54] P. Azaria, E. Boulat, and P. Lecheminant, Phys. Rev. B **61**, 12112 (2000).
[55] C. Itoi, S. Qin, and I. Affleck, Phys. Rev. B **61**, 6747 (2000).
[56] A. M. Tsvelik, Phys. Rev. B **42**, 10499 (1990).
[57] R. Egger and A. O. Gogolin, Phys. Rev. Lett. **79**, 5082 (1997).
[58] G. Blumberg Phys. Lett. B **617**, 133 (2005).
[59] T. Vuletić, B. Korin-Hamzić, S. Tomić, B. Gorshunov, P. Haas, T. Rõõm, M. Dressel, J. Akimitsu, T. Sasaki, and T. Nagata, Phys. Rev. Lett. **90**, 257002 (2003).
[60] A. Rusydi, P. Abbamonte, H. Eisaki, Y. Fujimaki, G. Blumberg, S. Uchida, C. C. Kao, and G. A. Sawatzky (unpublished).
[61] A. Gozar, G. Blumberg, B. S. Dennis, B. S. Shastry, N. Motoyama, H. Eisaki, and S. Uchida, Phys. Rev. Lett. **87**, 197202 (2001).